Renewable and Sustainable Energy Reviews 81 (2018) 536–551

Contents lists available at ScienceDirect

Renewable and Sustainable Energy Reviews

journal homepage: www.elsevier.com/locate/rser

A review of ZnO nanoparticles as solar photocatalysts: Synthesis, mechanisms and applications

Chin Boon Ong[a], Law Yong Ng[b], Abdul Wahab Mohammad[a,c,*]

[a] Department of Chemical and Process Engineering, Faculty of Engineering and Built Environment, Universiti Kebangsaan Malaysia, UKM, 43600 Bangi, Selangor, Malaysia

[b] Department of Chemical Engineering, Lee Kong Chian Faculty of Engineering and Science, Universiti Tunku Abdul Rahman, Jalan Sungai Long, Bandar Sungai Long, Cheras, 43000 Kajang, Selangor, Malaysia

[c] Centre for Sustainable Process Technology (CESPRO), Faculty of Engineering and Built Environment, Universiti Kebangsaan Malaysia, UKM, 43600 Bangi, Selangor, Malaysia

ARTICLE INFO

Keywords:
Solar photocatalytic
Zinc oxide
Nanoparticles
Persistent organic pollutants

ABSTRACT

Persistent organic pollutants (POPs) are carbon-based chemical substances that are resistant to environmental degradation and may not be completely removed through treatment processes. Their persistence can contribute to adverse health impacts on wild-life and human beings. Thus, the solar photocatalysis process has received increasing attention due to its great potential as a green and eco-friendly process for the elimination of POPs to increase the security of clean water. In this context, ZnO nanostructures have been shown to be prominent photocatalyst candidates to be used in photodegradation owing to the facts that they are low-cost, non-toxic and more efficient in the absorption across a large fraction of the solar spectrum compared to TiO_2. There are several aspects, however, need to be taken into consideration for further development. The purpose of this paper is to review the photo-degradation mechanisms of POPs and the recent progress in ZnO nanostructured fabrication methods including doping, heterojunction and modification techniques as well as improvements of ZnO as a photocatalyst. The second objective of this review is to evaluate the immobilization of photocatalyst and suspension systems while looking into their future challenges and prospects.

1. Introduction

In recent years, implementation of water reclamation and reuse is gaining attention rapidly world-wide due to the water scarcity occurred as a result of climate change and poor water resource management (i.e. limited access to clean water resources and water demands exceed the available resources). Access to clean water is becoming an ever increasing problem in an expanding global economy and population countries [1]. One of the attractive solutions in response to water issues is implementation of wastewater reclamation and reuse projects to ensure a sustainable water development and management. However, concerns still arise from the fact that persistent organic pollutants (POPs) could still be present in treated water.

POPs are carbon-based chemical substances that are resistant to environment degradation and have been continuously released into the environment. POPs can cause severe harm to human beings and wildlife because of their poor biodegradability and carcinogenic characteristics in nature. Advanced treatment technologies are crucial to ensure that the reclaimed water is free of POPs. Various water treatment techniques have been employed to remove POPs from water streams including adsorption, membrane separation and coagulation [2]; however these processes only concentrate or change the recalcitrant organic pollutants from the water to solid phase. Additional cost and treatments are thus needed to treat the secondary pollutants and regenerate the adsorbents [3]. For this reason, advanced oxidation processes (AOPs) have been proposed for the elimination of recalcitrant organic pollutants, especially for those with low biodegradability. According to Capelo et al. [4], AOP is a process that involves in situ generation of highly potent chemical oxidants with the assistance of ozone (O_3), hydrogen peroxide (H_2O_2), Fenton's reagent, UV light or a catalyst. The generated hydroxyl radicals (·OH) are strong oxidants that are able to oxidize recalcitrant organic compounds. AOPs offer several advantages such as: (i) rapid degradation rate, (ii) mineralization of organic compounds to green products, (iii) ability to operate under ambient temperature and pressure, and (iv) reduction of the toxicity of organic compounds.

* Corresponding author at: Department of Chemical and Process Engineering, Faculty of Engineering and Built Environment, Universiti Kebangsaan Malaysia, UKM, 43600 Bangi, Malaysia.

E-mail addresses: yblwyw@hotmail.com (C.B. Ong), drawm@ukm.edu.my (A.W. Mohammad).

http://dx.doi.org/10.1016/j.rser.2017.08.020
Received 21 July 2016; Received in revised form 20 March 2017; Accepted 8 August 2017

AOP mechanisms can be classified as homogeneous or heterogeneous photocatalysis. Homogeneous photocatalysis employs Fenton's reagent, which is a mixture of hydrogen peroxide and an Fe^{2+} salt to produce hydroxyl radicals under UV irradiation at wavelengths above 300 nm [5]. In contrast, heterogeneous photocatalysis employs semiconductor oxides as a photocatalyst [6]. Among semiconductors, titanium dioxide (TiO_2) has been the most studied compound in past decades. Owing to its low production cost and good chemical stability, it has been widely employed in photo-degradation of organic compounds, such as those with a high loading of nitrogen-containing organic compounds [7], saturated hydrocarbons (alkanes) [8], aromatic hydrocarbons [9] , non-biodegradable azo dyes [10], volatile organic compounds [11] and pesticides [12] with a UV light source. As reported by Wang et al. [13], the application of TiO_2 using solar energy is highly restricted by its large band gap (3.2 eV) and low quantum efficiency. Considerable attempts such as doping [14], formation of nanocomposites [15], surface modification, dye sensitization [16], noble metal [17] and non-noble metal deposition [18] have been made toward extending photoresponse and photoactivity of TiO_2 in visible light region. Comparable to TiO_2, ZnO is an n-type semiconductor oxide but has not been well investigated in previous studies. ZnO has been proposed as an alternative photocatalyst to TiO_2 as it possess same band gap energy but exhibits higher absorption efficiency across a large fraction of the solar spectrum when compared to TiO_2 [19,20]. In order to evaluate the photosensitization of ZnO and TiO_2, Fenoll et al. [21] compared the photo-degradation of fungicides in leaching water using the ZnO and TiO_2 under solar irradiation and found non-stoichiometric of ZnO rendering it a better photocatalyst compared to TiO_2 under solar irradiation.

Although AOPs have been shown to be effective in batement of recalcitrant organic matter, there is still much room for improvement. Firstly, the cost related to AOPs is a notable criterium in determining the applicability of the process in water treatment plants. Expensive chemicals and electricity consumption may lead to high operational costs and limit the applicability of AOPs in water treatment plants. Secondly, the rate of the degradation/oxidation reaction is dependent on the production of hydroxyl radicals and regeneration of ions [22]. Without sufficient formation of hydroxyl radicals, the effectiveness of AOPs in batement of recalcitrant organic pollutants is diminished. Many attempts have been made in the past decade to enhance the generation rate of hydroxyl radicals to improve AOP treatments [23]. Thirdly, there is a great need for understanding the toxicity of the intermediates and mineralization products generated from AOP. In a work by Rodriguez et al. [24], nicotine removal by employing Fenton's Reagent was used to study the mineralization and toxicity of intermediates generated in AOPs. They found that there was incomplete mineralization even though 100% of the nicotine was removed and the toxicity of the intermediates generated (especially those at initial stage of the oxidation process) was 15 times more greater than the initial solution.

Due to the advances in using photocatalysis in the degradation of recalcitrant organic pollutants, this technique has been developed for photocatalytic membrane reactors in large scale applications. Semiconductor oxides to be used in heterogenous photocatalysis are typically either – suspended in the effluent to be treated or immobilized on a support. The inconvenience of slurry-type reactors, in which the semiconductor oxides are suspended in the effluent, is the requirement of an additional step to recover the photocatalyst; such a process is not required using an immobilized-type reactor. Integration of photocatalysis into a membrane process is an approach that promises a continuous operation in addition to a good photocatalyst recovery [25].

The merits of photocatalysts suspended in the aqueous solutions are: low pressure drop across the reactor, good mass transfer of pollutants from the bulk liquid phase onto active surface sites of photocatalysts, and provision of a better platform for pollutants adsorption and desorption process throughout the reaction [26]. To compensate for the cost limitation of recovering the photocatalyst, heterogeneous photocatalysis which utilizes solar irradiation has been proposed as a more cost-effective process that can be conducted without the need for an artificial, and often costly, irradiation source.

Recently, more and more papers on fabrication and implementation of photocatalyst have been published due to the advantages of photocatalysis process. Hence, a review about the selection of appropriate photocatalyst fabrication methods to obtain desired dimension of ZnO nanostructures based on specific application and suitability of solar photocatalytic system should be carried out to ease the implementation of this technology in a bigger scale. The main objectives of the current review is to evaluate the employment of ZnO nanoparticles as solar photocatalysts, application of ZnO nanoparticles in water treatment, solar-photodegradation mechanisms of zinc oxide photocatalysis, synthesis methods of ZnO nanoparticles, comparisons between photocatalytic membrane reactor and the suspended system, as well as future challenges and prospects of using ZnO nanoparticles in these processes. Advantages through understanding the properties and characteristics of the ZnO photocatalyst in this paper, produced under various fabrication and modification methods, can provide researchers with different perceptions towards photocatalysis results that can possibly be obtained when the ZnO photocatalysts are integrated into different treatment systems.

2. Fundamental and mechanism of zinc oxide photocatalysis

ZnO is a type of semiconductor having a broad direct band gap width (3.37 eV), large excitation binding energy (60 meV) and deep violet/borderline ultraviolet (UV) absorption at room temperature [27]. It is an excellent semiconductor oxide that possesses favorable excellent electrical, mechanical and optical properties [28], similar to TiO_2. In addition, ZnO not only has antifouling and antibacterial properties, but also good photocatalytic activity [29]. Furthermore, as reported by Liang et al. [30], the production cost of ZnO is up to 75% lower than that of TiO_2 and Al_2O_3 nanoparticles. Due to the advantages of ZnO over TiO_2, ZnO has been suggested to be used in heterogeneous photocatalysis. According to Herrmann et al. [31], the heterogeneous photocatalytic oxidation steps can be explained as shown in Fig. 1.

1. Organic pollutants diffuse from the liquid phase to the surface of ZnO.
2. Adsorption of the organic pollutants on the surface of ZnO.
3. Oxidation and reduction reactions in the adsorbed phase.
4. Desorption of the products.
5. Removal of the products from the interface region.

When ZnO is photo-induced by solar light with photonic energy ($h\upsilon$) equal to or greater than the excitation energy (E_g), e^- from the filled valence band (VB) are promoted to an empty conduction band (CB). This photo-induced process produces electron-hole (e^-/h^+) pairs as shown in (Eq. (1)). The electron-hole pairs can migrate to the ZnO surface and be involved in redox reactions as shown in (Eqs. (2)–(4)), wherein the H^+ reacts with water and hydroxide ions to produce hydroxyl radicals while e^- reacts with oxygen to produce superoxide

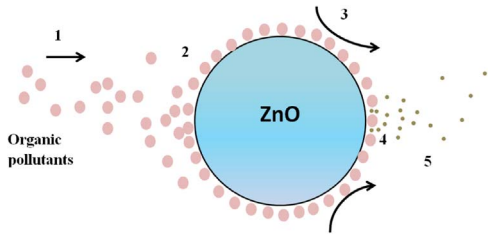

Fig. 1. Heterogeneous photocatalytic oxidation steps.
Adapted with permission from [31].

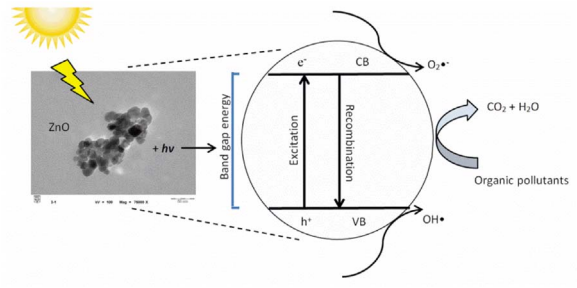

Fig. 2. Degradation of organic pollutants by ZnO in the presence of solar light. Adapted with permission from [32,33].

radical anions then hydrogen peroxide (Eq. (5)). Hydrogen peroxide will then react with superoxide radicals to form hydroxyl radicals (Eqs. (7)–(9)). Then, the resulting hydroxyl radicals, which are powerful oxidizing agents, will attack the pollutants adsorbed on the surface of ZnO to rapidly produce intermediate compounds. Intermediates will eventually be converted to green compounds such as CO_2, H_2O and mineral acids as shown in (Eq. (11)). Fig. 2 illustrates the redox reaction occurring during photocatalysis. Hence, the mechanism of photodegradation of organic compounds in the presence of solar radiation via redox reaction can be summarized as follows [32,33]:

$$ZnO \xrightarrow{h\upsilon} ZnO(e^-_{(CB)}) + (h^+_{(VB)}) \quad (1)$$

$$ZnO(h^+_{(VB)}) + H_2O \rightarrow ZnO + H^+ + OH\bullet \quad (2)$$

$$ZnO(h^+_{(VB)}) + OH^- \rightarrow ZnO + OH\bullet \quad (3)$$

$$ZnO(e^-_{(CB)}) + O_2 \rightarrow ZnO + O_2\bullet^- \quad (4)$$

$$O_2\bullet^- + H^+ \rightarrow HO_2\bullet \quad (5)$$

$$HO_2\bullet + HO_2\bullet \rightarrow H_2O_2 + O_2 \quad (6)$$

$$ZnO(e^-_{(CB)}) + H_2O_2 \rightarrow OH\bullet + OH^- \quad (7)$$

$$H_2O_2 + O_2\bullet^- \rightarrow OH\bullet + OH^- + O_2 \quad (8)$$

$$H_2O_2 + h\upsilon \rightarrow 2OH\bullet \quad (9)$$

$$\text{Organic pollutants} + OH\bullet \rightarrow \text{Intermediates} \quad (10)$$

$$\text{Intermediates} \rightarrow CO_2 + H_2O \quad (11)$$

As mentioned earlier, ZnO has been shown that to exhibit higher absorption efficiency across a larger fraction of solar spectrum compared to TiO_2. The photoactivity of a catalyst is governed by its ability to create photogenerated electron-hole pairs. The major constraint of ZnO as a photocatalyst, however, is the rapid recombination rate of photogenerated electron-hole pairs, which perturbs the photodegradation reaction. Additionally, it has also been noted that the solar energy conversion performance of ZnO is affected by its optical absorption ability, which has been associated with its large band gap energy. Therefore, intense efforts have been made to improve the optical properties of ZnO by minimizing the band gap energy and inhibiting the recombination of photogenerated electron-hole pairs. In the forthcoming discussion, ZnO synthesis methods and the effect of various modification methods (such as tuning the microstructure, doping and coupling two semiconductors) to improve the performance of ZnO in photocatalysis will be discussed in detail.

3. ZnO nanostructure material

3.1. Classification of ZnO

Nanostructures of ZnO are very important for photocatalytic reaction because it will determine their applications in various fields. A suitable nanostructure of ZnO will enable higher efficiency of process and enhance the recovery of photocatalyst during post-treatment stage. Various previous studies have been aimed at the production of ZnO with different nanostructures [34–36]. Nanostructures of ZnO can be

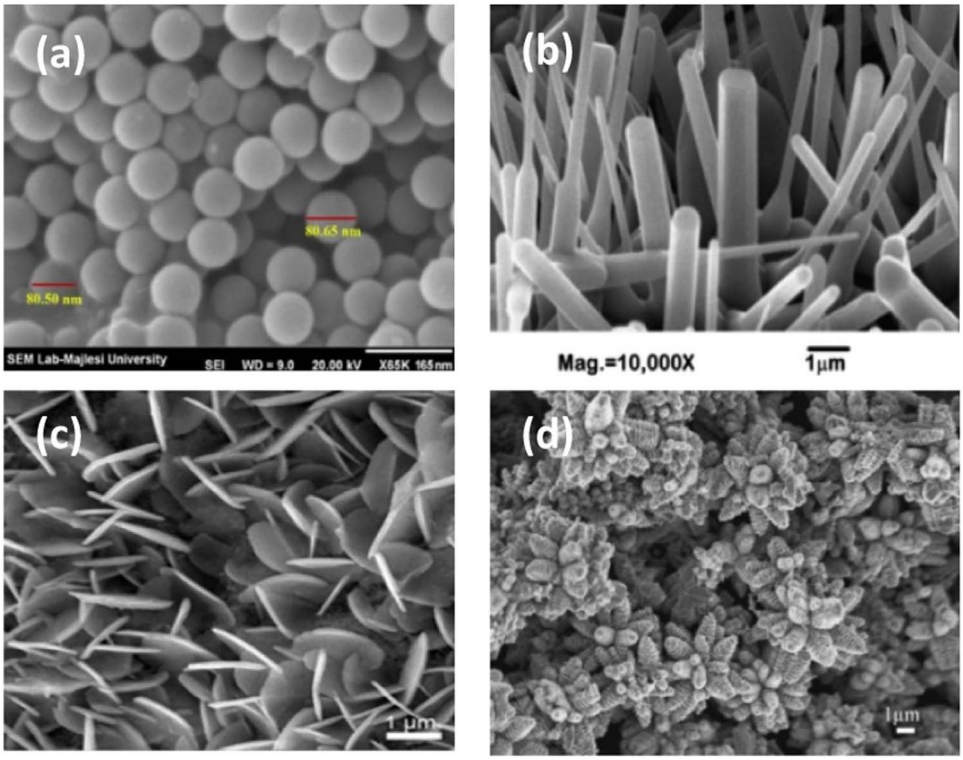

Fig. 3. FESEM and SEM images for (a) 0D, (b) 1D, (c) 2D, (d) 3D zinc oxides. Adapted with permission from [39–42].

divided into zero-dimensional (0D), one-dimensional (1D), two-dimensional (2D) and three-dimensional (3D). Each of these nanostructures can be subdivided into quantum dots arrays, elongated arrays, planar arrays and ordered structures respectively. Fig. 3 shows the morphologies of zinc oxides having different dimensions. 1D ZnO arrays include nanorods, nanofibres, nanowires, nanotubes and nanoneedles. Examples of ZnO nanostructures in 2D and 3D arrays are nanosheets and nanoflowers, respectively. ZnO-based nanomaterials have been employed in a number of emerging applications, especially in photovoltaics, electronic and photocatalytic processes owing to their high stability, good mechanical strength and high bulk of electron mobility. It has been reported that nanosized ZnO quantum dots can be incorporated into a fluorescent probe as a sensing receptor for the detection of copper (II) ions in water owing to their outstanding characteristics such as high quantum yield and stability [37]. 1D ZnO has widespread potential application in electronics, optoelectronics and gas sensing. Desai et al. [38] conducted mechanical strength tests on ZnO nanowires and discovered that the nanowires possess outstanding fracture strain, making nanowire good candidate for nanoscale sensors and actuators.

As mentioned earlier, the photoactivity of a photocatalyst is affected by its specific surface area. The large specific surface area and polar faces possessed by 2D ZnO [43] make ZnO nanosheets superior candidates for photocatalysis. The large specific surface area of ZnO enables more contaminants to be adsorbed onto its active surface and thus lead to more pollutants being attacked by hydroxyl radicals. The chain reaction that occurs at the surface enhances the degradation rate of the contaminants to produce non-toxic products. Another study by Luo et al. [44] reported that 3D nanoflowers showed a higher sensitivity in gas ethanol sensing compared to 1D and 2D nanostructures due to fact that nanoflowers have larger surface-to-volume ratios compared to nanostructures of other dimensionalities. This finding indicates that the capabilities of gas sensors are highly dependent on the morphology of materials. Additionally, ZnO nanoflowers also possesses better light scattering properties when compared to nanorods [45]. In another study, Xie et al. [46] fabricated nanoflower arrays of ZnO by incorporating ZnO nanowires on polystyrene spheres that attached together with a ZnO seed layer. This approach combined the advantages of 1D and 3D ZnO materials and contributed to a higher specific surface area. This advanced approach has made 3D nanoflowers become a promising material in solar applications such as fabrication of dye-sensitized solar cells. Table 1 shows the advantages and disadvantages of different ZnO nanostructures in photocatalytic applications. High surface areas offered by nanoparticles make it a popular choice in solar photocatalysis, as more pollutants could be easily adsorbed and a higher rate of degradation can be achieved. It has also been reported that the lower crystallinity and more defects in nanowires is an advantage in photocatalytic applications. This could be due to the hydroxyl groups bound on the defects (i.e. oxygen and surface defects) promoting the trapping of photoinduced electron-hole pairs and thus enhancing their separation [47].

3.2. Synthesis of ZnO nanostructure

There are various approaches for the synthesis of ZnO nanostructures. These synthesis methods can be divided into solution-based and vapor phase approaches. Band-gap energies and charge carrier separation of semiconductor oxides are size, crystal phase and crystallinity dependent. Researchers [49] have predicted that the bandgap energy is inversely proportional to the size of semiconductor compounds based on an established model. This implies that good control of preparation conditions determines the efficiency of photocatalysis.

Among ZnO nanomaterial synthesis methods, the solution-based approach is the simplest and least energy consuming. Through this synthesis route, the morphology of the nanostructures can be easily controlled by manipulating the experimental factors such as type of solvents, starting materials and reaction conditions [50]. This simple approach also offers better control of the sizes of nanostructures. Solution-based approaches to synthesize ZnO nanostructures including hydrothermal, sol-gel, precipitation, microemulsion, solvothermal, electrochemical deposition process, microwave, polyol, wet chemical method, flux methods and electrospinning [51–61]. Among these methods, the sol-gel technique is the most attractive method for ZnO nanostructure synthesis because of its low production cost, high reliability, good repeatability, simplicity of process, low process temperature, ease of control of physical characteristics and morphology of nanoparticles, good compositional homogeneity and optical properties [62,63]. In this context, ongoing research has modified the existing sol-gel technique by using only water as solvent [64]. For instance, Ciciliati et al. [65] fabricated Fe-doped ZnO nanoparticles by using a modified sol-gel method. The obtained Fe-doped ZnO nanoparticles by using this modified sol-gel method were found to be comparable with a previous study [66] that used ethanol as a solvent implying that the modified sol-gel method managed to produce a good quality of nanostructure materials but at a lower production cost.

On the other hand, vapor phase approaches have also been used to produce nanostructured materials; these processed include thermal evaporation [67], pulsed laser deposition [68], physical vapor deposition [69], chemical vapor deposition [70], metal-organic chemical vapor deposition (MOCVD) [71], plasma enhanced chemical vapor deposition (PECVD) [72] and molecular beam epitaxy (MBE) [73]. Among them, some methods utilize metal catalysts to control the growth of nanostructures; however, Tang et al. [74], managed to fabricate ZnO nanorods with good crystallinity and optical quality without the addition of any metal catalysts. They controlled the growth mechanism of ZnO by manipulating the initial growth temperature of samples, leading to the formation of different nucleation layers for Zn adsorption. Selection of ZnO synthesis method mainly depends on the dimension of nanostructures desired. For example, sol-gel method and PECVD have been utilized in the fabrication of 2D nanostructures. The PECVD method has proved that lower temperatures are sufficient to create the films-compared to sol-gel method [75]. Table 2 shows the effect of different fabrication methods on zinc oxide characteristics.

Table 1
Advantages and disadvantages of different ZnO nanostructures used in photocatalytic applications.
Source: Adapted with permission from [48].

	Advantages	Disadvantages
Nanoparticles	Can be easily suspended in a solution Outstanding performance owing to their large surface areas	Easily form agglomerates in solution, which contributes to reduced effective surface area Post-treatment for catalyst removal is required Complete recovery of catalyst is difficult
Nanowires	Growth could be easily carried out on most substrates Consists of large effective surface area compared to nano-thin films Post-treatment to remove catalyst is not required Lower crystallinity and more defects	Growth conditions are highly restricted Lower surface area compared to nanoparticles
Nano-thin film	Can be coated on certain substrates Post-treatment to remove catalyst is not required	Performance is restricted by small surface area

Table 2
The effect of fabrication methods on zinc oxide characteristics.

Fabrication	Starting materials	Morphology	Particle size, nm	Ref.
Microwave-assisted hydrothermal	Zinc nitrate-6-hydrate, zinc acetate dehydrate, hydrazine hydrate and ammonia	Low microwave power: needle shape High microwave power: flower-shape	50–150	[60]
Electrochemical	Zn electrode, oxalic acid dihydrate purified, potassium chloride, sodium hydroxide and nitric acid.	Combination of spherical and cylindrical particles	$L_{cylindrical}$: 150–200 $D_{spherical}$: 50–100	[76]
Solvothermal	Zinc acetylacetonate monohydrate,Triethanolamine, absolute ethanol and 1-octanol	Ethanol with TEA: Spherical shape Ethanol without TEA: Rod shape	D_{sphere} ~ 20 L_{rod} ~ 100	[77]
Sonochemical	Zinc nitrate hexahydrate, potassium hydroxide and cetyltrimethylammonium bromide	Flakes shape	200–400 wide and a few nm thick	[78]
Chemical vapor deposition	Zinc acetate di-hydrate, ethanol	Nanorod shape	Average diameter (90) and length (564)	[79]
Co-precipitation	Tetrahydrated zinc nitrate, ammonium hydroxide	Crystal shape	20–40	[80]
Wet chemical	Zinc chloride, sodium hydroxide	Nanodisc	300–500	[81]
Microemulsion	Ethyl benzene acid sodium salt (EBS), dodecyl benzene sulfonic acid sodium salt (DBS), zinc acetate dihydrate, xylene, hydrazine and ethanol	Nanorod	D_{EBS}: 80 D_{DBS}:300	[54]
Sol-gel	Zinc acetate dihydrate, oxalic acid dihydrate, ammonia, hydrochloric acid and absolute ethanol	Spherical shape	20	[82]

4. Improvement of ZnO as photocatalyst

4.1. Metal/non-metal doping

ZnO has a tetrahedral bonding configuration and it possesses large ionicity at the borderline between that of covalent and ionic semiconductors. As a result, ZnO possesses a large bandgap energy. ZnO can form a crystal in three different forms: hexagonal wurtzite, cubic zincblende and rocksalt [83]. ZnO hexagonal wurtzite is thermodynamically the most stable at ambient conditions. Cubic zincblende, however, can be stabilized by growing ZnO on cubic substrates. ZnO will exist in the rocksalt structure only at relatively high pressures [84]. Fig. 4 shows the crystalline structure of ZnO. ZnO is generally an intrinsically n-type semiconductor with the presence of intrinsic defects such as oxygen vacancies (V_O), zinc interstitials (Zn_i), and zinc vacancies (V_{Zn}), which will affect its optical properties and electrical behavior [85]. It has been noted that a greater V_O can provide more electron charge carriers. In Zhang et al. [86] studied the intrinsic doping asymmetry of ZnO via microscopic equilibrium mechanism and revealed that n-type ZnO can be easily obtained via intrinsic or extrinsic dopants. The major challenges of ZnO semiconductor fabrication are the difficulties in obtaining a stable and reproducible p-type ZnO. Limitations of asymmetric doping are due to the facts that:

(i) ZnO is n-type at Zn-rich conditions;
(ii) ZnO cannot be used to dope p-type via native defect such as zinc vacancy and oxygen interstitials; and
(iii) Electron-hole radiative recombination at the V_O acted as the source of the green luminescence were found.

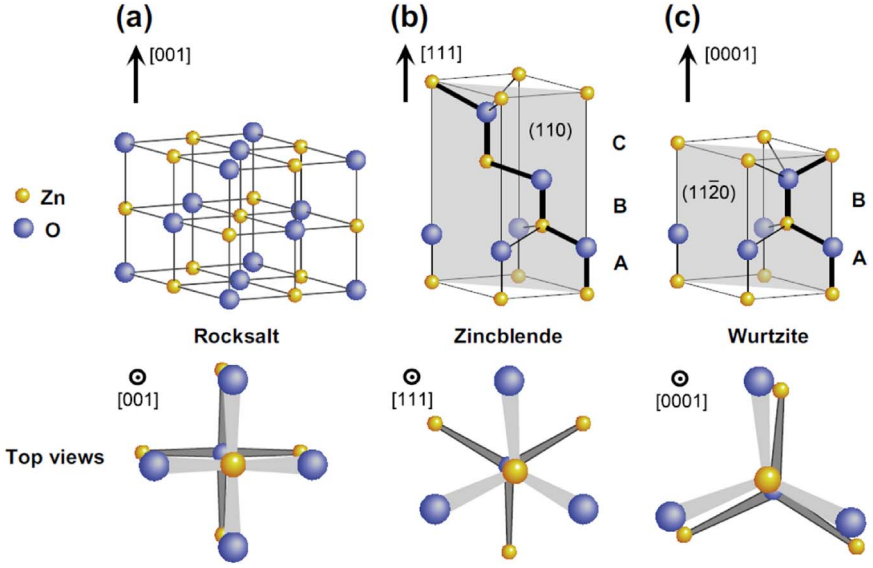

Fig. 4. Stick and ball representation of ZnO crystal structures: (a) cubic rocksalt (B1), (b) cubic zincblende (B3) and (c) hexagonal wurtzite (B4). Adapted with permission from [84].

When ZnO is under Zn-rich conditions, a self-compensation effect can easily occur. The native donor defects that are readily available from V_O, Zn_i, or Zn_O will compensate for native acceptor defects (O_i or V_{Zn}), thus, promoting the formation of n-type rather than p-type ZnO [87].

The high quality of p-type ZnO is optimal for various applications due to its high radiative stability. In Duan et al. [88] succeed in fabricating high quality Ag-N dual-doped p-type ZnO by using the sol-gel method. Among the fabricating methods (i.e. mono-doping, co-doping and dual-doping), the dual-doping method appeared to be vital for synthesize p-type ZnO. Apart from this, co-doping has started to gain extensive attention due to the different nature of dopants capable of tuning the optical properties of photocatalysts [89].

As mentioned before, photocatalytic reactions are mainly governed by bandgap energy and hydroxyl radicals. The main drawback for ZnO semiconductors as photocatalysts is their low-charge separation efficiency. Doping has thus been adopted to modify the physical and chemical properties of ZnO by incorporating impurities such as metals or non-metals, to shift the valence band energy of ZnO upward and narrowing the bandgap energy to the ultraviolet-visible region [90]. Recent studies have demonstrated that non-metal dopants such as nitrogen, carbon, sulfur and fluorine can shift the bandgap of ZnO by substituting V_O, thus introducing greater oxygen vacancy defects on the surface of nanoparticles. More specifically, C, F, O and N can diffuse through the lattice interstices and bind to the atoms via oxidation process owing to their extremely small sizes [91]. Carbon is a prominent candidate for a non-metal dopant for in semiconductors owing its high mechanical strength, good chemical resistance and special electronic properties [92]. In addition, doping also can contribute to a greater production of OH• radicals, thus, lead to a higher degradation efficiency of organic pollutants [93]. This was explained by the facts that the dopants can act as electron scavengers and prevent the recombination of electron-hole pairs, thus, free the positive hole (H^+) of photocatalyst (which is significant for the formation of OH• radicals) [94,95].

Recently, compounds like transition metals, rare earth metals, noble metals and other metals have shown advantages in tuning the morphology of ZnO in photocatalytic applications as well as other specific applications. Metal doping of ZnO can improve the photoactivity of catalysts by increasing the trapping site of the photo-induced charge carriers and thus decrease the recombination rate of photo-induced electron-hole pairs [96]. In order to decrease the bandgap energy of photocatalysts, metal dopants such as Ce, Nd, Cu and Al have been used in applications in dye degradation and gas sensing [97–100]. Yun et al. [101] have shown that higher loads of organic compounds could be adsorbed on Al-doped ZnO compared to pure ZnO based on the high light harvesting efficiency. On the other hand, it has been reported that Sn could be used to enhance the electrical conductivity of ZnO by substituting the Zn^{2+} ions without causing any large lattice distortion [102]. Another study by Zhu et al. [103] has reported that the incorporation of metal ions such as Fe^{3+}, can contribute to more oxygen defects on ZnO along with an increase in the charge density of ZnO, which subsequently can induce higher performance of the nanostructure. Fig. 5 displays the distribution of O, Zn and Fe in the Fe-doped ZnO nano-arrays. Similar work by Wang et al. [104] has endeavored to demonstrate that Ag-doped ZnO has a greater specific surface area of nanoparticles and greater lattice deficiency. Metal-doped ZnO, prepared using Mn and Co through co-precipitation method, was previously used in treating methyl orange via photocatalytic experiments [105]. Degradation and adsorption of methyl orange onto the heterogenous catalysts were shown to be greatly affected by the solution pH. According to that work, 12 at% was the optimal dopant concentration to be used in which the best degradation efficiency was recorded by Mn-doped ZnO catalyst at pH 4 or acidic condition. Table 3 shows various types of dopants and fabrication methods that were previously employed to synthesize ZnO nanostructures as well as their photocatalytic applications. Although metal dopants offer many advantages, non-metal dopants offer lower cost compared to metal dopant. Further studies may be needed to explore the trends, performance and characteristics of ZnO doping in detail.

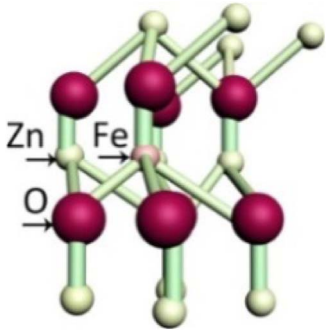

Fig. 5. Ball-and-stick model of crystal structure of Fe-doped ZnO. Adapted with permission from [103].

As previously discussed, non-metal/metal doping have been widely deployed to improve the charge separation of photocatalyst. However, a recent paper reviewed that over-doping could attribute to the reduction of ZnO photodegradation efficiency [106]. This is probably due to the excess dopants that act as trapping sites for both electrons and holes and thus inhibits the generation of hydroxyl radicals which are important for the degradation of recalcitrant organic pollutants.

4.2. ZnO coupling with other semiconductors

Coupling of two semiconductors is an approach that involves coupled semiconductor metal oxides such as M_xO_y/Me_zO_t (where M and Me represent the metal type and x, y, z, and t are the oxidation states in these metal oxides) [107]. Nanocomposites are preferable in several applications, especially for photocatalysis, because of their higher light absorption, better suppression of photoinduced electron-hole pair recombination and increased charge separation. Lin and Chiang [108] have shown that the increased charge separation was due to an extended lifetime of charge carriers by inter-particle electron transfer between the conduction bands of nanocomposites leading to a larger number of electrons involved in a photo-degradation reaction. These superior properties are ascribed to a stepwise energy-level structure in the composite [109]. Another similar study by Nur et al. [110] has also shown that highly active photocatalysts can be obtained by coupling two semiconductors having different band gaps. Based on their proposed mechanism, relatively efficient charge separation may be achieved due to photoinduced electrons that are transferred away from the photocatalyst. Therefore, the heterostructure of nanocomposites serve as an attractive alternative for enhancing the photoactivity of photocatalysts. For ZnO coupled with other semiconductors, TiO_2/ZnO, SnO_2/ZnO, SnO_2/ZnO/TiO_2 and Co_3O_4/ZnO are the most investigated materials for photocatalytic processes [111–118]. Fig. 6 shows the photogenerated charge separation enhancement mechanism of a ZnO/$TiO_{2x}N_y$ nanocomposite. The electron from ZnO was transferred into valence band of $TiO_{2x}N_y$ whereas the photogenerated hole of $TiO_{2x}N_y$ was transferred to ZnO. The occurrence of such phenomena has suppressed the recombination of e^-/h^+ pairs by prolonging the life time of charge carriers.

Nanosized coupled ZnO/SnO_2 photocatalyst were previously studied for the degradation of methyl orange [120]. According to the work, photodegradation of methyl orange by nanosized coupled ZnO/SnO_2 photocatalyst reached their maximum when the Sn content was about 33.3 mol%. This has been explained by their heterojunctions in coupled ZnO/SnO_2 photocatalyst.

Table 3
Application of doped ZnO as photocatalysts.

Type of dopants	Dopants	Fabrication method	Photocatalytic application	Targeted pollutants	Ref.
Transition metals	Mn	Microwave assisted hydrothermal	Dye degradation	MB	[152]
		Sol-gel	Dye degradation	Direct Yellow 27 & Acid Blue 129	[153]
		Wet chemical	Dye degradation	MB	[154]
		Co-precipitation	Dye degradation	MB	[155]
	Mo	Sol-gel	Dye degradation	Direct Yellow 27 and Acid Blue 129	[153]
	Cu	Sol-gel	Dye degradation	MB, MO	[156,157]
		Co-precipitation	Dye degradation	DB 71 dye, CV	[158,159]
		Vapor transport	Dye degradation	Rz	[160]
	Co	Co-precipitation	Dye degradation	RhB	[161]
	Fe	Sol-gel	Aromatic organic compound degradation	2-chlorophenol	[66]
	Ag	Spray pyrolysis	Dye degradation	AO7	[162]
		Laser-induction	Dye degradation	MB	[163]
		Photo reduction, chemical reduction or polyacrylamide-gel methods	Phenolic compounds	4-nitrophenol	[164]
	Pd	Sol-gel	Dye degradation	MO	[165]
		Incipient wetness impregnation	Disinfection	*E. coli*	[166]
	Y	Microwave irradiation	Dye degradation	MB	[167]
	Hf	Sol-gel	Dye degradation	MB	[168]
Alkaline earth	Mg	Auto combustion	Dye degradation	MO	[169]
		Co-precipitation	Endocrine disrupting chemicals	4-chlorophenol	[170]
		Solid state reaction	Pharmaceutical compounds	Alprazolam	[171]
Other metals	Sn	Solid-state synthesis	Dye degradation	MO	[172]
	Ni	Sol-gel	Dye degradation	MG	[173]
	Bi	Parallel flaw precipitation	Dye degradation	MO	[174]
	Al	Plasma spraying	Dye degradation	MB	[175]
Rare earth metal	Ce	Sonochemical	Dye degradation	MB	[97]
		Reflux method	Dye degradation	MB	[96]
		Hydrothermal	Dye degradation	MB	[176]
		Sonochemical wet impregnation	Pesticide degradation	Cyanide	[177]
	Nd	Sonochemical	Dye degradation	MB	[98]
		Wet chemical	Dye degradation	RhB	[178]
		Hydrothermal	Dye degradation	MO	[179]
	Eu	Precipitation	Dye degradation	MO	[180]
	Sm	Chemical solution route	Aromatic organic compound degradation	2,4-dichlorophenol	[181]
		Solvothermal	Aromatic organic compound degradation	Phenol	[182]
	La	Precipitation/mechanical milling	Dye degradation	MB	[183]
		Co-precipitation	Pesticide degradation	MCP	[184]
	Gd	Sonochemical	Dye degradation	AO7	[185]
Non-metal	C	Hydrothermal	Endocrine disrupting chemicals degradation	Bisphenol A	[92]
			Dye degradation	RhB	[186]
	S	Mechanochemical synthesis/thermal decomposition	Endocrine disrupting chemicals degradation	Resorcinol	[187]
	N	Calcined the mixture of commercial ZnO and NH_4NO_3	Organic compounds degradation	Formaldehyde	[188]
		Sol-gel	Dye degradation	MB	[189]
			Aromatic organic compound degradation	Phenol	[189]
		Solvothermal	Dye degradation	MO	[190]
		Modified non-basic solution/annealing in NH_3	Dye degradation	RhB	[90]

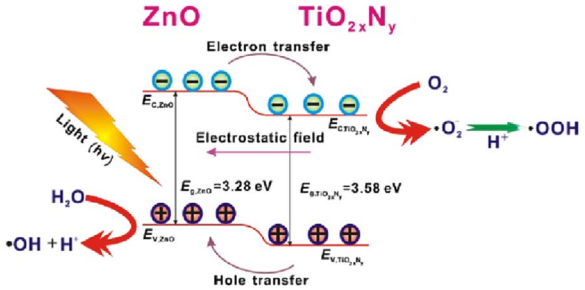

Fig. 6. Photogenerated charge separation mechanism of ZnO coupled with $TiO_{2x}N_y$. Adapted with permission from [119].

4.3. Coupling of nanocarbon component to ZnO

Heterojunction photocatalysts are also effective at enhancing the properties of ZnO photocatalyst. It has been reported by Chang et al. [121] that the heterostructure of photocatalysts, combined with the merits of different compounds including light absorption, charge separation, and charge transfer between differents kind of semiconductors can cause rapid photogenerated charge separation. Carbon nanostructures play pivotal roles in the development of nanocomposites. In the last decade, it has been reported that the heterojunction of ZnO with carbon nanotubes can enhance the performance of nanocomposites by acting as electron scavenging agents [122].

Graphene (from the carbon family), has been of considerable

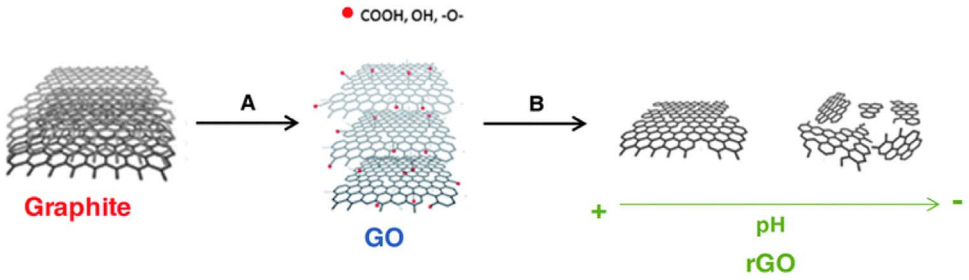

Fig. 7. Synthesis of reduced graphene oxide (rGO): (A) oxidation of graphite to graphene oxide (B) reduction of graphene oxide to reduced-graphene oxide. Adapted with permission from [134].

interest in many applications such as photocatalysis, gas sensing, photovoltaic devices, and fuel cells in the last few years due to its excellent electrical conductivity, high surface area, high electron mobility and chemical stability [123]. Graphene is a sp^2 carbon-based nanomaterial in a single atom thick sheet which is arranged in a hexagonal honeycomb lattice distribution. Single-layer graphene exhibits rather high specific surface area (2630 $m^2\ g^{-1}$), Young's modulus (1.0 terapascals), thermal conductivity (~ 5000 $W\ m^{-1}\ g^{-1}$) and mobility charge carriers (200,000 $cm^2\ V^{-1}\ s^{-1}$) [124–127]. These optimal properties are mainly attributed to the presence of functional groups such as hydroxyl, epoxide, carboxylic and carbonyl groups. As can be seen in Fig. 7, the interplanar spacing between graphite is increased through oxidation processes using Hummer's method. Oxidation into graphene oxide (GO) perturbs the electrical conductivity, creating an excellent electrical insulator [128]. GO can be reduced into reduced-graphene oxide (rGO) by manipulating the pH of GO in solution and followed by a thermal treatment. Recent works have revealed that the heterostructure of ZnO/GO has greater carrier transport efficiency due to the graphene encapsulation, specific surface area and electrical transport properties [129,130]. A sol-gel method has been used by Fu et al. [131] to prepare ZnO decorated graphene and they found that the adsorption of dyes during the photocatalytic process was increased along with higher loading of graphene implying that graphene can also be used as adsorbent in water treatment. Enhancement in adsorption of organic pollutants probably is due to π–π conjugation between organic pollutants and the sp^2 regions of rGO according to a report work [132]. Further studies on graphene adsorption behavior under different conditions are needed to achieve an optimum removal efficiency. ZnO coupled with rGO should improve the photocatalytic degradation of organic pollutants. However, rGO loading exceeding the optimum dosage will lead to a lower degradation efficiency, which could be explained by high photo-absorbing and scattering [133].

Cysteine capped ZnO/graphene oxide composite, which was previously prepared using co-precipitation method, showed improvement in photodegradation of Rhodamine B [135]. Optimum addition of GO in cysteine capped ZnO photocatalyst showed an increase in the degradation efficiency at about 98.13% within 45 min.

4.4. Crystal growth and shape control

To improve the photoactivity, various methods have been used to modify the morphology, size and growth of ZnO. It has been noted that the photoactivity can be altered by varying the surface lattice plane and surface area of photocatalysts [118]. For example, capping agents have been successfully used to alter the morphology of ZnO nanoparticles. In previous work [53], triethanolamine (TEA)-capped ZnO exhibited triangular-like morphology, whereas tetraethylammonium bromide (TEABr)-capped ZnO showed a free morphology. Likewise, the morphology of ZnO can be altered by manipulating the molar ratios of precursors [136], as suggested by Gupta et al. [137], who showed that the shape and size of ZnO particles were correlated to the concentration of OH^- ions. Examples of chemical reactions for ZnO synthesis via the chemical approach are as follows:

$$Zn^{2+} + 2OH^- \rightarrow Zn(OH)_2 \quad (12)$$

$$Zn(OH)_2 \rightarrow ZnO + H_2O \quad (13)$$

$$Zn(OH)_2 + 2OH^- \rightarrow [Zn(OH)_4]^{2-} \quad (14)$$

$$[Zn(OH)_4]^{2-} \rightarrow ZnO + H_2O + 2OH^- \quad (15)$$

Fig. 8 shows that low and high concentration of OH^- result in ZnO growth in uniform and anisotrophic directions, respectively. In contrast, intermediate concentrations of OH^- has contributed to simultaneous uniform and anisotrophic growth, thus resulting in the formation of uniformity in the shape of nanoparticles and nanorod nanostructures.

Another recent work have revealed that the speed of precursor (sodium hydroxide) being added to the zinc acetate solution could contribute to different growth mechanisms of ZnO nanostructures [138]. According to that work, when a slow addition rate of OH^- was performed, the growth of ZnO nanostructures favored a uniform direction. When both precursors (sodium hydroxide and zinc acetate) solution were mixed at the same time, however, would cause the reaction to perform faster. In this case, growth along the [0001] direction is more favorable due to the excess of OH^-, thus, lead to nanosheet formation. The most interesting finding was when relatively slow addition rate of OH^- was performed, the growth along the [0001] direction was restricted, which contributed to the formation of hexagonal prism as shown in Fig. 9. Among those different shapes of ZnO nanostructures, spherical ZnO nanostructures were reported to exhibit the highest degradation rate of organic pollutants ascribed to their large oxygen vacancies.

Effect of ZnO crystallite sizes towards the photocatalytic activity has been well-linked to their band-gap energy. This has been proven in a previous work [139], in which ZnO crystallite sizes of 4.8 and 31.4 nm are having band-gap energy of 3.29 and 3.18 eV, respectively. On the other hand, another recent paper has reported that a high dielectric constant of the solvent used during fabrication could lead to a smaller crystallite size of ZnO [139]. For instance, methanol that possesses higher dielectric constant (32) than ethanol (25) and propanol (21) produced smaller crystallite size of ZnO (4.8 nm) compared to propanol (14.7 nm), but not for ethanol based solvent (4.1 nm). This is due to the fact that dielectric constant of the solvent can alter the

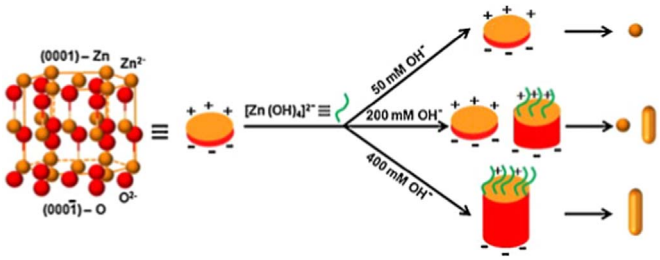

Fig. 8. Effect of OH^- concentration towards the mechanisms of ZnO formation. Adapted with permission from [137].

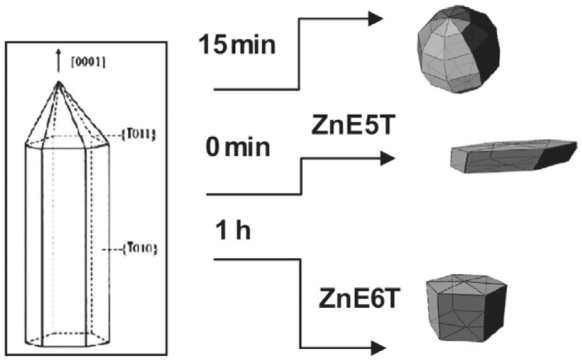

Fig. 9. Effect of precursor adding rate towards the mechanisms of ZnO formation. Adapted with permission from [138].

interparticle forces and thus affects the growth and crystallite size of ZnO. Similar finding was also reported in a recent work [140].

4.5. Surface modification of ZnO

Owing to the existence of Zn–O–Zn bonds in ZnO nanoparticles, agglomeration occurs readily, thus strongly limiting ZnO nanoparticle applications [141]. Surface modification may be the best approach for ensuring better dispersion by preventing the agglomeration of ZnO. In addition, surface modification has also been used to tune the ultraviolet and visible light photoluminescence, as the chemical and physical properties of ZnO nanoparticles can be modified via chemical surface modification through chemical treatment [142], coating [141], grafting polymerization [72], ligand exchange [143] and self-assembly techniques [144]. Chemical treatment is an approach that utilizes coupling agents (e.g. trimethoxyvinyl silane and oleic acid) to modify the surface of nanoparticles. Modified ZnO fabricated by Hong et al. [145] through grafting polymerization has shown better dispersion in organic matrix compared to bare ZnO nanoparticles.

Ligand molecules (i.e. polymeric ligands and monomeric ligands) are also common capping agents used in the coating method to prevent the aggregation and control the growth of nanoparticles. The ligand layer acts as an insulating barrier and blocks the charge transport between neighboring nanoparticles before recombinations can occur [146]. Recently, stabilization of ZnO nanoparticles through coating method using polymeric ligands has proved to be better than monomeric ligands. This is due to the presence of steric and electrostatic forces that were used to stabilize the ZnO in the polymeric ligands but in the latter, only electrostatic repulsive forces can contribute to the ZnO stabilization [147]. Coating method manages to improve the dispersion of nanoparticles in the matrix, however, this method may impede the photocatalysis at the same time [141]. In order to simultaneously stabilize and enhance the performance of nanoparticles, ligand exchange – (a method where the attached ligand molecules on the surface of photocatalyst can be exchanged with other ligand molecules) could be a more preferable approach. In this context, Kango et al. [148] has reported that ligand molecules should be exchanged with more suitable ligands in order to enhance the transfer of electrons by lowering the separation effects.

In contrast, flower-like ZnO structures were successfully synthesized by controlling the molar ratio of Zn^{2+} and OH^- ions. Previous research has revealed that excess OH^- may lead to the formation of the $[Zn(OH)4]^{2-}$ complex. Subsequent dehydration of the $[Zn(OH)4]^{2-}$ complex favored formation of nanosheet array from particles. Flower-like ZnO structures then form due to the tendency of nanosheets to minimize their surface energy [149]. Poly(vinyl pyrrolidone) was previously used as an intermediate to anchor ZnO on solvent exfoliated graphene [150]. Poly(vinyl pyrrolidone) was reported to decrease the surface free energy through its attachment on the ZnO surface thus lead to slow growth of the facets and provided good dispersion of the nanoparticles. Photocatalytic activity of produced photocatalyst in the degradation of Reactive Black 5 was 97% at a rate constant of 0.0199 min^{-1}. Fig. 10 shows a schematic drawing of surface modification methods. It can be clearly seen in Fig. 10(a) that polymer grafting can penetrate the organic matrix and separate the aggregated nanoparticles.

5. Comparison of photocatalyst immobilization and suspension system

The hybrid photocatalytic-membrane process is a promising technology that does not require complicated recovery of photocatalysts after water treatment. Photocatalytic reactions using this hybrid technology utilize stationary nanostructured photocatalysts to enhance the absorption of photons and reactants so that the catalyst does not need to be suspended in solution [191]. The photocatalytic process is gaining popularity owing to the fact that nanostructured photocatalysts possess high efficiency in degrading persistent organic pollutants into readily biodegradable compounds. Photocatalysis coupled to membrane processes, such as ultrafiltration and nanofiltration, have been deployed in many applications such as the removal of endocrine compound (i.e. estrone) [192], pharmaceutically active compounds (i.e. diclofenac) [193], fungicides in leaching water (i.e. cyprodinil and fludioxonil) [21] and Congo red dye treatment [194]. To date, there is a significant development in photocatalytic membrane reactors (PMR) in which sunlight is utilized in the system instead of UV light. The substitution in light source is more favorable owing to its lower electricity cost and wider application in area with easy access to sunlight.

While the hybrid photocatalytic-membrane process is a promising technology in water treatment, there are some technical constraints which need to be overcome before it can be implemented in full scale in various fields. First, rather few studies have been carried out on the stability of polymer membranes in PMR. Second, there are only few studies that have related the kinetic models and mass transfer limitations that affect the performance of the separation in PMR systems. Third, studies on the performance of PMR systems should be conducted using the real water samples instead of synthetic proxies to investigate the real conditions of the system, including the effects of colloidal particles towards the stability of photocatalytic performance. The established advantages of PMR with a photocatalyst immobilized on a membrane substrate are [195,196]:

- No extra photocatalyst recovery steps.
- Stable flux and low flux-decline rate.
- Contaminants could be decomposed, either in feed or in permeate.
- Mitigation of membrane fouling due to the decomposition of organic contaminants and enhanced hydrophilicity of the modified membrane.

Photocatalytic membranes are utilized in separation processes due to their superior properties such as anti-fouling, anti-microbial, superhydrophilicity, concurrent photocatalytic oxidation and separation compared to conventional membranes [197,198]. There are two configurations of PMR with photocatalytic membranes:

(i) membrane with photoactive layer formed on a porous non-photoactive support and
(ii) membrane with non-photoactive layer formed on a porous photoactive support.

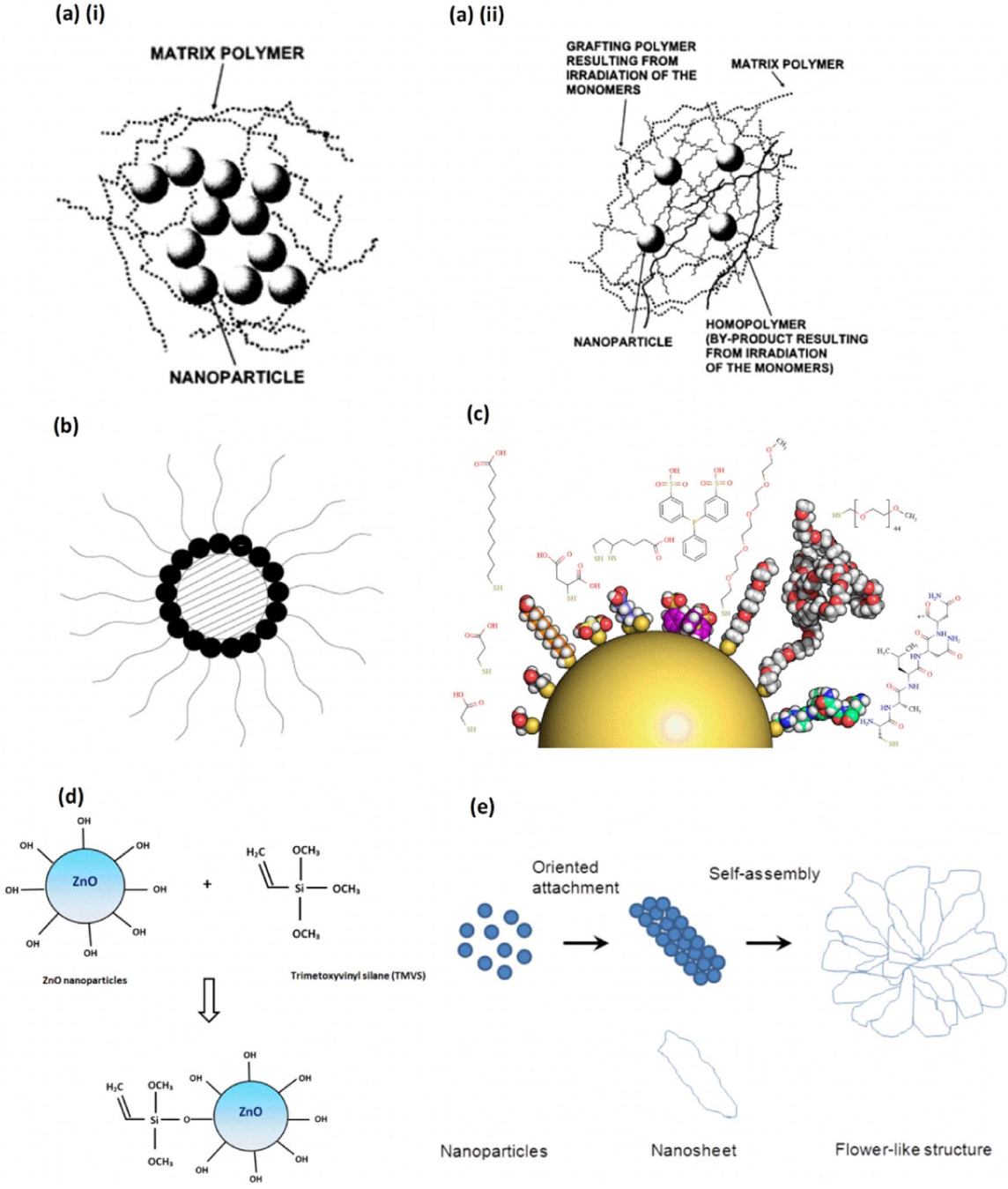

Fig. 10. Schematic drawing of (a) (i) agglomerated nanoparticles, (ii) grafted nanoparticles dispersed in polymer matrix, (b) coating, (c) ligand exchange, (d) chemical treatment and (e) self-assembly. Adapted with permission from [141–143,149,151].

In the former, the irradiation source is placed on the feed side and in the latter, the irradiation source is placed on the permeate side, as depicted in Fig. 11. The main advantages of the membrane configuration with the photoactive layer formed on a porous non-photoactive support are fouling mitigation and increase flux of permeate due to the fact that the organic compounds can be decomposed before being transported through the membrane. Membranes with a non-photoactive layer formed on a porous photoactive support are less popular in comparison to the configuration on a non-photoactive support. In the case of the photoactive support, photodegradation is carried out on the permeate side and thus causes a reduction in permeate water quality [25]. Immobilization of photocatalyst particles on membranes faces some technical challenges. Song et al. [199] has reported that a photocatalytic membrane can undergo damage after a long irradiation period. Thus, through investigations of durability, and ultraviolet light and hydroxyl radical resistance of polymer membranes must be conducted in order to overcome the damage of polymer membranes.

In contrast to immobilized systems, suspended reactor systems can be defined as a degradation process in which nanoparticles are suspended in water/wastewater. Therefore, catalyst separation and recovery is an essential step for catalyst recycling. Hu et al. [200] compared the decoloring methyl orange (MO) under sunlight using a ZnO photocatalyst immobilization and suspension system. They found that 98% of the decoloration of MO was attained within 40 min of

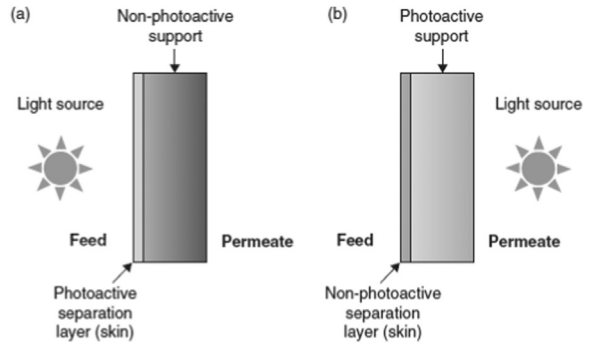

Fig. 11. Configurations of PMR with photocatalytic membranes (a) membrane with photoactive layer formed on a porous non-photoactive support and (b) membrane with non-photoactive layer formed on a porous photoactive support.
Adapted with permission from [195].

sunlight irradiation in a slurry type reactor, whereas only 74% of decoloration was achieved after 6 h of irradiation using the ZnO immobilized on a polymeric membrane because the slurry type reactor offers a large surface area of photocatalyst when compared to photocatalyst immobilized on a membrane. Table 4 shows the comparison between the suspended and immobilized system in the photocatalytic degradation process. It can be concluded that both systems possess their own merits and disadvantages; therefore, the selection of an appropriate system should be based on the requirements of a specific application.

6. Future challenges and prospects

The implementation of solar-driven photocatalysis is believed to be able to perform better than conventional methods in the degradation of recalcitrant organic pollutants. In order to enhance the feasibility of this technology in the future, extensive efforts are needed to further overcome some challenges. First, photocatalytic degradation studies must be performed using the organic pollutant of interest rather than a proxy. In the literature, there are plenty of studies using dye as model organic pollutant for photocatalytic degradation. However, dyes can be easily removed and their removal can be easily attained compared to other organic pollutants such as pesticides and endocrine distrupting compounds. A deeper understanding of the degradation mechanisms and the interaction between the photocatalysts and other organic pollutants is still required. Second, more improvements may still be made in the development of nanostructures. In most cases, the efficiency of photocatalytic reactions is governed by the photocatalysts. Even though current techniques are able to fabricate good photocatalysts (in terms of high surface area, small particle size, longer lifespan of charge carrier and so forth), further work is needed in this area. Thirdly, researchers need to further investigate the quality and performance of photocatalytic membranes if PMR is chosen. There are several practical problems arising from the fabrication of photocatalytic membranes, such as the durability of polymer membrane, leaching of photocatalysts from supports and production cost. Besides, there are also operating problems need to be overcoming such as loss and recovery of photocatalyst during post-treatment as well as photoactivity of recycled photocatalyst. Furthermore, more extensive work is needed to develop and verify the mathematical models for photocatalytic operations/systems for water/wastewater treatment in order to predict their quantum yield, kinetics and optimum condition of the process.

7. Conclusions

ZnO nanostructures have been shown to be a potential candidate as photocatalyst for solar-driven photodegradation process of persistent organic pollutants. This is attributed to its low production cost (75% lower in comparison to TiO_2 and Al_2O_3), non-toxic and ability to absorb larger fraction of solar spectrum compared to TiO_2. From the examples of fabrication methods presented in previous sections, it can seen that zinc oxide characteristics such as dimension (0D, 1D, 2D and 3D), morphology and particle size are affected by its fabrication methods. Among the fabrication methods, solution-based approaches are favorable due to its ability to provide a good platform to control growth mechanisms of ZnO nanostructures, which has been demonstrated experimentally through a well-controlled molar ratios of percursors. There are various methods that have been attempted to enhance photoresponse of ZnO nanostructures. Bandgap energy is reported to play important factor in determining the photoactivity of ZnO in application. It can be concluded that techniques such as metal/non-metal doping, ZnO coupling with other semiconductors, coupling of nanocarbon can improved ZnO as a photocatalyst in photodegradation application. These techniques will enhance their performance by shifting the bandgap energy, suppressing the recombination rate of electron-hole pairs, increasing charge separation efficiency, improving production rate of hydroxyl radicals, producing smaller particle size with high specific surface area, and allowing better dispersion in medium. It was experimentally proved that ZnO nanoparticle with the highest specific surface area showed the highest removal ratio towards the degradation of Rhodamine B (84%, 78% and 75% when using spherical, nanosheet and hexagonal prismatic ZnO nanoparticles, respectively). From the examples of PMR system presented above, it was proven that high efficiency of photocatalytic reaction could be achieved with the appropriate selection of desired nanostructures in terms of synthesis method as well as proper photocatalytic system. In order to provide more stable and better performance in degradation of recalcitrant organic pollutants in larger scale of application, future research should look into overcoming the weak points of ZnO and the practical issues that are still existing.

Table 4
Comparison between suspended and immobilized system in photocatalytic degradation process.

	Suspended system	Immobilized system	Ref.
Post-separation of catalysts	Extra recovery step is needed	No extra recovery step required	[195]
Active surface area	Large active surface area for adsorption and degradation	Limited active surface area available for adsorption and degradation	[201]
Quantum yield	High quantum yield	Half the quantum yield of suspended system	[202]
Stability of performance	Not consistent for repeatable reaction owing to the loss of nanoparticles	More stable for repeatable reaction	[200,203]
Electric energy per order (EE/O)	Requires lower electric energy compared to immobilized system to achieve same degradation	Require higher electric energy compared to suspended system to achieve same degradation	[204]
Aeration	No significant effect on degradation	Synergistic effect on the efficiency of system owing to oxygen increased the mass transfer of the system	[205]

Acknowledgement

The authors are grateful for the financial support from Grant ICONIC-2013-002 (Universiti Kebangsaan Malaysia). One of the authors C.B. Ong, wishes to acknowledge the Ministry of Education Malaysia for supporting her postgraduate study via MyBrain.

References

[1] Hartley TW. Public perception and participation in water reuse. Desalination 2006;187:115–26. http://dx.doi.org/10.1016/j.desal.2005.04.072.
[2] Plumlee MH, Larabee J, Reinhard M. Perfluorochemicals in water reuse. Chemosphere 2008;72:1541–7. http://dx.doi.org/10.1016/j.chemosphere.2008.04.057.
[3] Guo H, Lin K, Zheng Z, Xiao F, Li S. Sulfanilic acid-modified P25 TiO2 nanoparticles with improved photocatalytic degradation on Congo red under visible light. Dye Pigment 2012;92:1278–84. http://dx.doi.org/10.1016/j.dyepig.2011.09.004.
[4] Capelo-Martínez JL, Ximénez-Embún P, Madrid Y, Cámara C. Advanced oxidation processes for sample treatment in atomic spectrometry. TrAC Trends Anal Chem 2004;23:331–40. http://dx.doi.org/10.1016/S0165-9936(04)00401-7.
[5] Malato S, Blanco J, Vidal A, Richter C. Photocatalysis with solar energy at a pilot-plant scale: an overview. Appl Catal B Environ 2002;37:1–15.
[6] Wang Kuo-Hua, Tsai Huan-Hung, Hsieh Yung-Hsu. A study of photocatalytic degradation of trichloroethylene in vapor phase on TiO2 photocatalyst. Chemosphere 1998;36:2763–73. http://dx.doi.org/10.1016/S0045-6535(97)10235-1.
[7] Klare M, Scheen J, Vogelsang K, Jacobs H, Broekaert JA. Degradation of short-chain alkyl- and alkanolamines by TiO2- and Pt/TiO2-assisted photocatalysis. Chemosphere 2000;41:353–62. http://dx.doi.org/10.1016/S0045-6535(99)00447-6.
[8] Cermenati L, Dondi D, Fagnoni M, Albini A. Titanium dioxide photocatalysis of adamantane. Tetrahedron 2003;59:6409–14. http://dx.doi.org/10.1016/S0040-4020(03)01092-5.
[9] Ziolli RL, Jardim WF. Photochemical transformations of water-soluble fraction (WSF) of crude oil in marine waters: a comparison between photolysis and accelerated degradation with TiO2 using GC–MS and UVF. J Photochem Photobiol A Chem 2003;155:243–52. http://dx.doi.org/10.1016/S1010-6030(02)00397-0.
[10] Alaton IA, Balcioglu IA. Photochemical and heterogeneous photocatalytic degradation of waste vinylsulphone dyes: a case study with hydrolyzed Reactive Black 5. J Photochem Photobiol A Chem 2001;141:247–54. http://dx.doi.org/10.1016/S1010-6030(01)00440-3.
[11] Monneyron P, Manero M-H, Foussard J-N, Benoit-Marquié F, Maurette M-T. Heterogeneous photocatalysis of butanol and methyl ethyl ketone—characterization of catalyst and dynamic study. Chem Eng Sci 2003;58:971–8. http://dx.doi.org/10.1016/S0009-2509(02)00637-1.
[12] Autin O, Hart J, Jarvis P, MacAdam J, Parsons SA, Jefferson B. The impact of background organic matter and alkalinity on the degradation of the pesticide metaldehyde by two advanced oxidation processes: UV/H2O2 and UV/TiO2. Water Res 2013;47:2041–9. http://dx.doi.org/10.1016/j.watres.2013.01.022.
[13] Wang A, Teng Y, Hu X, Wu L, Huang Y, Luo Y, et al. Diphenylarsinic acid contaminated soil remediation by titanium dioxide (P25) photocatalysis: degradation pathway, optimization of operating parameters and effects of soil properties. Sci Total Environ 2016;541:348–55. http://dx.doi.org/10.1016/j.scitotenv.2015.09.023.
[14] Song M, Bian L, Zhou T, Zhao X. Surface ζ potential and photocatalytic activity of rare earths doped TiO2. J Rare Earths 2008;26:693–9. http://dx.doi.org/10.1016/S1002-0721(08)60165-9.
[15] Wang D, Wang Y, Li X, Luo Q, An J, Yue J. Sunlight photocatalytic activity of polypyrrole–TiO2 nanocomposites prepared by “in situ” method. Catal Commun 2008;9. http://dx.doi.org/10.1016/j.catcom.2007.10.027.
[16] Macák JM, Tsuchiya H, Ghicov A, Schmuki P. Dye-sensitized anodic TiO2 nanotubes. Electrochem Commun 2005;7. http://dx.doi.org/10.1016/j.elecom.2005.08.013.
[17] An H, Zhou J, Li J, Zhu B, Wang S, Zhang S, et al. Deposition of Pt on the stable nanotubular TiO2 and its photocatalytic performance. Catal Commun 2009;11. http://dx.doi.org/10.1016/j.catcom.2009.09.020.
[18] Wang X, Zhang S, Peng B, Wang H, Yu H, Peng F. Enhancing the photocatalytic efficiency of TiO2 nanotube arrays for H2 production by using non-noble metal cobalt as co-catalyst. Mater Lett 2016;165. http://dx.doi.org/10.1016/j.matlet.2015.11.103.
[19] Qiu R, Zhang D, Mo Y, Song L, Brewer E, Huang X, et al. Photocatalytic activity of polymer-modified ZnO under visible light irradiation. J Hazard Mater 2008;156:80–5. http://dx.doi.org/10.1016/j.jhazmat.2007.11.114.
[20] Yogendra K, Naik S, Mahadevan KM, Madhusudhana N. A comparative study of photocatalytic activities of two different synthesized ZnO composites against Coralene red F3BS dye in presence of natural solar light. J Environ Sci Res 2011;1:11–5.
[21] Fenoll J, Ruiz E, Hellín P, Flores P, Navarro S. Heterogeneous photocatalytic oxidation of cyprodinil and fludioxonil in leaching water under solar irradiation. Chemosphere 2011;85:1262–8. http://dx.doi.org/10.1016/j.chemosphere.2011.07.022.
[22] Torrades F, Pérez M, Mansilla HD, Peral J. Experimental design of Fenton and photo-Fenton reactions for the treatment of cellulose bleaching effluents. Chemosphere 2003;53:1211–20. http://dx.doi.org/10.1016/S0045-6535(03)00579-4.
[23] Muñoz I, Rieradevall J, Torrades F, Peral J, Domènech X. Environmental assessment of different solar driven advanced oxidation processes. Sol Energy 2005;79:369–75. http://dx.doi.org/10.1016/j.solener.2005.02.014.
[24] Rodriguez S, Santos A, Romero A. Effectiveness of AOP's on abatement of emerging pollutants and their oxidation intermediates: nicotine removal with Fenton's reagent. Desalination 2011;280:108–13. http://dx.doi.org/10.1016/j.desal.2011.06.055.
[25] Molinari R, Palmisano L, Loddo V, Mozia S, Morawski AW. 21 – photocatalytic membrane reactors: configurations, performance and applications in water treatment and chemical production. Handb Membr React 2013:808–45. http://dx.doi.org/10.1533/9780857097347.4.808.
[26] Alfano O, Bahnemann D, Cassano A, Dillert R, Goslich R. Photocatalysis in water environments using artificial and solar light. Catal Today 2000;58:199–230. http://dx.doi.org/10.1016/S0920-5861(00)00252-2.
[27] Choi K, Kang T, Oh S-G. Preparation of disk shaped ZnO particles using surfactant and their PL properties. Mater Lett 2012;75. http://dx.doi.org/10.1016/j.matlet.2012.02.031.
[28] Gharoy Ahangar E, Abbaspour-Fard MH, Shahtahmassebi N, Khojastehpour M, Maddahi P. Preparation and characterization of PVA/ZnO nanocomposite. J Food Process Preserv 2015;39:1442–51. http://dx.doi.org/10.1111/jfpp.12363.
[29] Al-Fori M, Dobretsov S, Myint MTZ, Dutta J. Antifouling properties of zinc oxide nanorod coatings. Biofouling 2014;30:871–82. http://dx.doi.org/10.1080/08927014.2014.942297.
[30] Liang S, Xiao K, Mo Y, Huang X. A novel ZnO nanoparticle blended polyvinylidene fluoride membrane for anti-irreversible fouling. J Memb Sci 2012;394:184–92. http://dx.doi.org/10.1016/j.memsci.2011.12.040.
[31] Herrmann J-M. Heterogeneous photocatalysis: fundamentals and applications to the removal of various types of aqueous pollutants. Catal Today 1999;53:115–29. http://dx.doi.org/10.1016/S0920-5861(99)00107-8.
[32] Rajamanickam D, Shanthi M. Photocatalytic degradation of an organic pollutant by zinc oxide – solar process. Arab J Chem 2016;9:S1858–S1868. http://dx.doi.org/10.1016/j.arabjc.2012.05.006.
[33] Rauf MA, Ashraf SS. Fundamental principles and application of heterogeneous photocatalytic degradation of dyes in solution. Chem Eng J 2009;151:10–8. http://dx.doi.org/10.1016/j.cej.2009.02.026.
[34] Meng Y, Lin Y, Yang J. Synthesis of rod-cluster ZnO nanostructures and their application to dye-sensitized solar cells. Appl Surf Sci 2013;268:561–5. http://dx.doi.org/10.1016/j.apsusc.2012.12.171.
[35] Manzoor U, Kim DK. Size control of ZnO nanostructures formed in different temperature zones by varying Ar flow rate with tunable optical properties. Phys E Low-Dimens Syst Nanostruct 2009;41:500–5. http://dx.doi.org/10.1016/j.physe.2008.09.012.
[36] Jimenez-Cadena G, Comini E, Ferroni M, Vomiero A, Sberveglieri G. Synthesis of different ZnO nanostructures by modified PVD process and potential use for dye-sensitized solar cells. Mater Chem Phys 2010;124:694–8. http://dx.doi.org/10.1016/j.matchemphys.2010.07.035.
[37] Ng SM, Wong DSN, Phung JHC, Chua HS. Integrated miniature fluorescent probe to leverage the sensing potential of ZnO quantum dots for the detection of copper(II) ions. Talanta 2013;116:514–9. http://dx.doi.org/10.1016/j.talanta.2013.07.031.
[38] Desai AV, Haque MA. Mechanical properties of ZnO nanowires. Sens Actuators A Phys 2007;134:169–76. http://dx.doi.org/10.1016/j.sna.2006.04.046.
[39] Zavar S. A novel three component synthesis of 2-amino-4H-chromenes derivatives using nano ZnO catalyst. Arab J Chem 2017;10:S67–S70. http://dx.doi.org/10.1016/j.arabjc.2012.07.011.
[40] Hassan NK, Hashim MR, Bououdina M. One-dimensional ZnO nanostructure growth prepared by thermal evaporation on different substrates: ultraviolet emission as a function of size and dimensionality. Ceram Int 2013;39:7439–44. http://dx.doi.org/10.1016/j.ceramint.2013.02.088.
[41] Ju D, Xu H, Zhang J, Guo J, Cao B. Direct hydrothermal growth of ZnO nanosheets on electrode for ethanol sensing. Sens Actuators B Chem 2014;201:444–51. http://dx.doi.org/10.1016/j.snb.2014.04.072.
[42] Yue S, Lu J, Zhang J. Synthesis of three-dimensional ZnO superstructures by a one-pot solution process. Mater Chem Phys 2009;117. http://dx.doi.org/10.1016/j.matchemphys.2009.05.010.
[43] Jang ES, Won J-H, Hwang S-J, Choy J-H. Fine tuning of the face orientation of ZnO crystals to optimize their photocatalytic activity. Adv Mater 2006;18:3309–12. http://dx.doi.org/10.1002/adma.200601455.
[44] Luo J, Ma SY, Sun AM, Cheng L, Yang GJ, Wang T, et al. Ethanol sensing enhancement by optimizing ZnO nanostructure: from 1D nanorods to 3D nanoflower 2014;137. http://dx.doi.org/10.1016/j.matlet.2014.08.108.
[45] Qi L, Li H, Dong L. Simple synthesis of flower-like ZnO by a dextran assisted solution route and their photocatalytic degradation property. Mater Lett 2013;107. http://dx.doi.org/10.1016/j.matlet.2013.06.054.
[46] Xie F, Centeno A, Zou B, Ryan MP, Riley DJ, Alford NM. Tunable synthesis of ordered zinc oxide nanoflower-like arrays. J Colloid Interface Sci 2013;395:85–90. http://dx.doi.org/10.1016/j.jcis.2012.12.028.
[47] Zhang X, Qin J, Xue Y, Yu P, Zhang B, Wang L, et al. Effect of aspect ratio and surface defects on the photocatalytic activity of ZnO nanorods. Sci Rep 2014;4:4596. http://dx.doi.org/10.1038/srep04596.
[48] Zhang Y, Ram MK, Stefanakos EK, Goswami DY. Synthesis, characterization, and applications of ZnO nanowires. J Nanomater 2012;2012:1–22. http://dx.doi.org/10.1155/2012/624520.

[49] Li M, Li JC. Size effects on the band-gap of semiconductor compounds. Mater Lett 2006;60. http://dx.doi.org/10.1016/j.matlet.2006.01.032.
[50] Banerjee P, Chakrabarti S, Maitra S, Dutta BK. Zinc oxide nano-particles – sonochemical synthesis, characterization and application for photo-remediation of heavy metal. Ultrason Sonochem 2012;19:85–93. http://dx.doi.org/10.1016/j.ultsonch.2011.05.007.
[51] Wang F, Qin X, Guo Z, Meng Y, Yang L, Ming Y. Hydrothermal synthesis of dumbbell-shaped ZnO microstructures. Ceram Int 2013;39:8969–73. http://dx.doi.org/10.1016/j.ceramint.2013.04.096.
[52] Fang Y, Li Z, Xu S, Han D, Lu D. Optical properties and photocatalytic activities of spherical ZnO and flower-like ZnO structures synthesized by facile hydrothermal method. J Alloy Compd 2013;575:359–63. http://dx.doi.org/10.1016/j.jallcom.2013.05.183.
[53] Chandrasekaran P, Viruthagiri G, Srinivasan N. The effect of various capping agents on the surface modifications of sol–gel synthesised ZnO nanoparticles. J Alloy Compd 2012;540:89–93. http://dx.doi.org/10.1016/j.jallcom.2012.06.032.
[54] Lim SK, Hwang S-H, Kim S, Park H. Preparation of ZnO nanorods by microemulsion synthesis and their application as a CO gas sensor. Sens Actuators B Chem 2011;160:94–8. http://dx.doi.org/10.1016/j.snb.2011.07.018.
[55] Wan L, Yan S, Feng J, Yang Z, Fan X, Li Z, et al. Solvothermal synthesis of core–shell ZnO hollow microhemispheres. Colloids Surf A Physicochem Eng Asp 2012;396:46–50. http://dx.doi.org/10.1016/j.colsurfa.2011.12.039.
[56] Jiao S, Zhang K, Bai S, Li H, Gao S, Li H, et al. Controlled morphology evolution of ZnO nanostructures in the electrochemical deposition: from the point of view of chloride ions. Electrochim Acta 2013;111:64–70. http://dx.doi.org/10.1016/j.electacta.2013.08.050.
[57] Yue S, Lu J, Zhang J. Controlled growth of well-aligned hierarchical ZnO arrays by a wet chemical method. Mater Lett 2009;63. http://dx.doi.org/10.1016/j.matlet.2009.06.055.
[58] Ushio M, Sumiyoshi Y. Synthesis of ZnO single crystals by the flux method. J Mater Sci 1993;28:218–24. http://dx.doi.org/10.1007/BF00349054.
[59] Wu H, Pan W. Preparation of zinc oxide nanofibers by electrospinning. J Am Ceram Soc 2006;89:699–701. http://dx.doi.org/10.1111/j.1551-2916.2005.00735.x.
[60] Hasanpoor M, Aliofkhazraei M, Delavari H. Microwave-assisted synthesis of zinc oxide nanoparticles. Procedia Mater Sci 2015;11:320–5. http://dx.doi.org/10.1016/j.mspro.2015.11.101.
[61] Lee S, Jeong S, Kim D, Hwang S, Jeon M, Moon J. ZnO nanoparticles with controlled shapes and sizes prepared using a simple polyol synthesis. Superlattices Microstruct 2008;43:330–9. http://dx.doi.org/10.1016/j.spmi.2008.01.004.
[62] Vafaee M, Ghamsari MS. Preparation and characterization of ZnO nanoparticles by a novel sol–gel route. Mater Lett 2007;61. http://dx.doi.org/10.1016/j.matlet.2006.11.089.
[63] Köse H, Karaal Ş, Aydın AO, Akbulut H. A facile synthesis of zinc oxide/multiwalled carbon nanotube nanocomposite lithium ion battery anodes by sol–gel method. J Power Sources 2015;295:235–45. http://dx.doi.org/10.1016/j.jpowsour.2015.06.135.
[64] Davar F, Salavati-Niasari M. Synthesis and characterization of spinel-type zinc aluminate nanoparticles by a modified sol–gel method using new precursor. J Alloy Compd 2011;509:2487–92. http://dx.doi.org/10.1016/j.jallcom.2010.11.058.
[65] Ciciliati MA, Silva MF, Fernandes DM, de Melo MAC, Hechenleitner AAW, Pineda EAG. Fe-doped ZnO nanoparticles: synthesis by a modified sol–gel method and characterization. Mater Lett 2015;159. http://dx.doi.org/10.1016/j.matlet.2015.06.023.
[66] Ba-Abbad MM, Kadhum AAH, Mohamad AB, Takriff MS, Sopian K. Visible light photocatalytic activity of Fe^{3+}-doped ZnO nanoparticle prepared via sol–gel technique. Chemosphere 2013;91:1604–11. http://dx.doi.org/10.1016/j.chemosphere.2012.12.055.
[67] Jiang DY, Zhao JX, Zhao M, Liang QC, Gao S, Qin JM, et al. Optical waveguide based on ZnO nanowires prepared by a thermal evaporation process. J Alloy Compd 2012;532:31–3. http://dx.doi.org/10.1016/j.jallcom.2012.03.114.
[68] Ma X, Zhang J, Lu J, Ye Z. Room temperature growth and properties of ZnO films by pulsed laser deposition. Appl Surf Sci 2010;257:1310–3. http://dx.doi.org/10.1016/j.apsusc.2010.08.057.
[69] Ouyang W, Zhu J. Catalyst-free synthesis of macro-scale ZnO nanonail arrays on Si substrate by simple physical vapor deposition. Mater Lett 2008;62. http://dx.doi.org/10.1016/j.matlet.2007.12.051.
[70] Zhang N, Yi R, Shi R, Gao G, Chen G, Liu X. Novel rose-like ZnO nanoflowers synthesized by chemical vapor deposition. Mater Lett 2009;63. http://dx.doi.org/10.1016/j.matlet.2008.11.046.
[71] Lee C-H, Kim D-W. Thickness dependence of microstructure and properties of ZnO thin films deposited by metal-organic chemical vapor deposition using ultrasonic nebulization. Thin Solid Films 2013;546:38–41. http://dx.doi.org/10.1016/j.tsf.2013.05.029.
[72] Hu P, Han N, Zhang D, Ho JC, Chen Y. Highly formaldehyde-sensitive, transition-metal doped ZnO nanorods prepared by plasma-enhanced chemical vapor deposition. Sens Actuators B Chem 2012;169:74–80. http://dx.doi.org/10.1016/j.snb.2012.03.035.
[73] Wang C, Chen Z, Hu H, Zhang D. Effect of the oxygen pressure on the microstructure and optical properties of ZnO films prepared by laser molecular beam epitaxy. Phys B Condens Matter 2009;404:4075–82. http://dx.doi.org/10.1016/j.physb.2009.07.165.
[74] Tang H, Zhu L, Ye Z, He H, Zhang Y, Zhi M, et al. Synthesis of two kinds of ZnO nanostructures by vapor phase method. Mater Lett 2007;61. http://dx.doi.org/10.1016/j.matlet.2006.06.085.
[75] Sobczyk-Guzenda A, Pietrzyk B, Szymanowski H, Gazicki-Lipman M, Jakubowski W. Photocatalytic activity of thin TiO2 films deposited using sol–gel and plasma enhanced chemical vapor deposition methods. Ceram Int 2013;39:2787–94. http://dx.doi.org/10.1016/j.ceramint.2012.09.046.
[76] Anand V, Srivastava VC. Zinc oxide nanoparticles synthesis by electrochemical method: optimization of parameters for maximization of productivity and characterization. J Alloy Compd 2015;636:288–92. http://dx.doi.org/10.1016/j.jallcom.2015.02.189.
[77] Šarić A, Štefanić G, Dražić G, Gotić M. Solvothermal synthesis of zinc oxide microspheres. J Alloy Compd 2015;652:91–9. http://dx.doi.org/10.1016/j.jallcom.2015.08.200.
[78] Ghosh S, Majumder D, Sen A, Roy S. Facile sonochemical synthesis of zinc oxide nanoflakes at room temperature. Mater Lett 2014;130. http://dx.doi.org/10.1016/j.matlet.2014.05.112.
[79] Laurenti M, Garino N, Porro S, Fontana M, Gerbaldi C. Zinc oxide nanostructures by chemical vapour deposition as anodes for Li-ion batteries. J Alloy Compd 2015;640:321–6. http://dx.doi.org/10.1016/j.jallcom.2015.03.222.
[80] Kumar VR, Wariar PRS, Prasad VS, Koshy J. A novel approach for the synthesis of nanocrystalline zinc oxide powders by room temperature co-precipitation method. Mater Lett 2011;65. http://dx.doi.org/10.1016/j.matlet.2011.04.015.
[81] Samanta PK, Mishra S. Wet chemical growth and optical property of ZnO nanodiscs. Opt – Int J Light Electron Opt 2013;124:2871–3. http://dx.doi.org/10.1016/j.ijleo.2012.08.066.
[82] Ba-Abbad MM, Kadhum AAH, Mohamad AB, Takriff MS, Sopian K. Optimization of process parameters using D-optimal design for synthesis of ZnO nanoparticles via sol–gel technique. J Ind Eng Chem 2013;19:99–105. http://dx.doi.org/10.1016/j.jiec.2012.07.010.
[83] Morkoç H, Özgür Ü General properties of ZnO. Zinc oxide. Weinheim, Germany: Wiley-VCH Verlag GmbH & Co. KGaA; n.d., p. 1–76. ⟨http://dx.doi.org/10.1002/9783527623945.ch1⟩.
[84] Özgür Ü, Avrutin V, Morkoç H. Chapter 16 – zinc oxide materials and devices grown by MBE. Mol Beam Epitaxy 2013:369–416. http://dx.doi.org/10.1016/B978-0-12-387839-7.00016-6.
[85] Boukos N, Chandrinou C, Travlos A. Zinc vacancies and interstitials in ZnO nanorods. Thin Solid Films 2012;520:4654–7. http://dx.doi.org/10.1016/j.tsf.2011.10.138.
[86] Zhang SB, Wei S-H, Zunger A. Intrinsic *n*-type versus *p*-type doping asymmetry and the defect physics of ZnO. Phys Rev B 2001;63:75205. http://dx.doi.org/10.1103/PhysRevB.63.075205.
[87] Collins TC, Hauenstein RJ. Fundamental properties of ZnO. Zinc Oxide Mater. Electron. Optoelectron. Device Appl. Chichester, UK: John Wiley & Sons, Ltd; 2011, p. 1–28. ⟨http://dx.doi.org/10.1002/9781119991038.ch1⟩.
[88] Duan L, Zhang W, Yu X, Jiang Z, Luan L, Chen Y, et al. Annealing effects on properties of Ag–N dual-doped ZnO films. Appl Surf Sci 2012;258:10064–7. http://dx.doi.org/10.1016/j.apsusc.2012.06.075.
[89] Mereu RA, Mesaros A, Vasilescu M, Popa M, Gabor MS, Ciontea L, et al. Synthesis and characterization of undoped, Al and/or Ho doped ZnO thin films. Ceram Int 2013;39:5535–43. http://dx.doi.org/10.1016/j.ceramint.2012.12.067.
[90] Yu Z, Yin L-C, Xie Y, Liu G, Ma X, Cheng H-M. Crystallinity-dependent substitutional nitrogen doping in ZnO and its improved visible light photocatalytic activity. J Colloid Interface Sci 2013;400:18–23. http://dx.doi.org/10.1016/j.jcis.2013.02.046.
[91] Di Valentin C, Pacchioni G. Trends in non-metal doping of anatase TiO2: B, C, N and F. Catal Today 2013;206:12–8. http://dx.doi.org/10.1016/j.cattod.2011.11.030.
[92] Bechambi O, Sayadi S, Najjar W. Photocatalytic degradation of bisphenol A in the presence of C-doped ZnO: effect of operational parameters and photodegradation mechanism. J Ind Eng Chem 2015;32:201–10. http://dx.doi.org/10.1016/j.jiec.2015.08.017.
[93] Nenavathu BP, Krishna Rao AVR, Goyal A, Kapoor A, Dutta RK. Synthesis, characterization and enhanced photocatalytic degradation efficiency of Se doped ZnO nanoparticles using trypan blue as a model dye. Appl Catal A Gen 2013;459:106–13. http://dx.doi.org/10.1016/j.apcata.2013.04.001.
[94] Sirelkhatim A, Mahmud S, Seeni A, Kaus NHM, Ann LC, Bakhori SKM, et al. Review on zinc oxide nanoparticles: antibacterial activity and toxicity mechanism. Nano-Micro Lett 2015;7:219–42. http://dx.doi.org/10.1007/s40820-015-0040-x.
[95] Hosseini SM, Sarsari IA, Kameli P, Salamati H. Effect of Ag doping on structural, optical, and photocatalytic properties of ZnO nanoparticles. J Alloy Compd 2015;640:408–15. http://dx.doi.org/10.1016/j.jallcom.2015.03.136.
[96] Rezaei M, Habibi-Yangjeh A. Simple and large scale refluxing method for preparation of Ce-doped ZnO nanostructures as highly efficient photocatalyst. Appl Surf Sci 2013;265:591–6. http://dx.doi.org/10.1016/j.apsusc.2012.11.053.
[97] Yayapao O, Thongtem S, Phuruangrat A, Thongtem T. Sonochemical synthesis, photocatalysis and photonic properties of 3% Ce-doped ZnO nanoneedles. Ceram Int 2013;39:S563–S568. http://dx.doi.org/10.1016/j.ceramint.2012.10.136.
[98] Yayapao O, Thongtem T, Phuruangrat A, Thongtem S. Ultrasonic-assisted synthesis of Nd-doped ZnO for photocatalysis. Mater Lett 2013;90. http://dx.doi.org/10.1016/j.matlet.2012.09.027.
[99] Song DM, Li JC. First principles study of band gap of Cu doped ZnO single-wall nanotube modulated by impurity concentration and concentration gradient. Comput Mater Sci 2012;65:175–81. http://dx.doi.org/10.1016/j.commatsci.2012.07.031.
[100] Ahmad M, Ahmed E, Zhang Y, Khalid NR, Xu J, Ullah M, et al. Preparation of highly efficient Al-doped ZnO photocatalyst by combustion synthesis. Curr Appl Phys 2013;13:697–704. http://dx.doi.org/10.1016/j.cap.2012.11.008.
[101] Yun S, Lee J, Chung J, Lim S. Improvement of ZnO nanorod-based dye-sensitized

solar cell efficiency by Al-doping. J Phys Chem Solids 2010;71:1724–31. http://dx.doi.org/10.1016/j.jpcs.2010.08.020.
[102] Phuruangrat A, Kongnuanyai S, Thongtem T, Thongtem S. Ultrasound-assisted synthesis, characterization and optical property of 0–3 wt% Sn-doped ZnO. Mater Lett 2013;91. http://dx.doi.org/10.1016/j.matlet.2012.09.091.
[103] Zhu D, Hu T, Zhao Y, Zang W, Xing L, Xue X. High-performance self-powered/active humidity sensing of Fe-doped ZnO nanoarray nanogenerator. Sens Actuators B Chem 2015;213:382–9. http://dx.doi.org/10.1016/j.snb.2015.02.119.
[104] Wang R, Xin JH, Yang Y, Liu H, Xu L, Hu J. The characteristics and photocatalytic activities of silver doped ZnO nanocrystallites. Appl Surf Sci 2004;227:312–7. http://dx.doi.org/10.1016/j.apsusc.2003.12.012.
[105] Saleh R, Djaja NF. Transition-metal-doped ZnO nanoparticles: synthesis, characterization and photocatalytic activity under UV light. Spectrochim Acta Part A Mol Biomol Spectrosc 2014;130:581–90. http://dx.doi.org/10.1016/j.saa.2014.03.089.
[106] Lee KM, Lai CW, Ngai KS, Juan JC. Recent developments of zinc oxide based photocatalyst in water treatment technology: a review. Water Res 2016;88:428–48. http://dx.doi.org/10.1016/j.watres.2015.09.045.
[107] Reza M. Coupled semiconductor metal oxide nanocomposites: types, synthesis conditions and properties. Adv. Compos. Mater. Med. Nanotechnol. InTech; 2011. ⟨http://dx.doi.org/10.5772/14357⟩.
[108] Lin C-C, Chiang Y-J. Preparation of coupled ZnO/SnO2 photocatalysts using a rotating packed bed. Chem Eng J 2012;181:196–205. http://dx.doi.org/10.1016/j.cej.2011.11.062.
[109] Johra FT, Jung W-G. RGO–TiO_2–ZnO composites: synthesis, characterization, and application to photocatalysis. Appl Catal A Gen 2015;491:52–7. http://dx.doi.org/10.1016/j.apcata.2014.11.036.
[110] Nur H, Misnon II, Wei LK. Stannic oxide-titanium dioxide coupled semiconductor lhotocatalyst loaded with polyaniline for enhanced photocatalytic oxidation of 1-octene. Int J Photoenergy 2007;2007:1–6. http://dx.doi.org/10.1155/2007/98548.
[111] Chiang Y-J, Lin C-C. Photocatalytic decolorization of methylene blue in aqueous solutions using coupled ZnO/SnO_2 photocatalysts. Powder Technol 2013;246:137–43. http://dx.doi.org/10.1016/j.powtec.2013.04.033.
[112] Yang G, Yan Z, Xiao T. Preparation and characterization of SnO_2/ZnO/TiO_2 composite semiconductor with enhanced photocatalytic activity. Appl Surf Sci 2012;258:8704–12. http://dx.doi.org/10.1016/j.apsusc.2012.05.078.
[113] Wang H, Baek S, Lee J, Lim S. High photocatalytic activity of silver-loaded ZnO-SnO_2 coupled catalysts. Chem Eng J 2009;146:355–61. http://dx.doi.org/10.1016/j.cej.2008.06.016.
[114] Zhang M, An T, Hu X, Wang C, Sheng G, Fu J. Preparation and photocatalytic properties of a nanometer ZnO–SnO_2 coupled oxide. Appl Catal A Gen 2004;260:215–22. http://dx.doi.org/10.1016/j.apcata.2003.10.025.
[115] Moradi S, Aberoomand-Azar P, Raeis-Farshid S, Abedini-Khorrami S, Givianrad MH. The effect of different molar ratios of ZnO on characterization and photocatalytic activity of TiO_2/ZnO nanocomposite. J Saudi Chem Soc 2016;20:373–8. http://dx.doi.org/10.1016/j.jscs.2012.08.002.
[116] Li C, Liu Q, Shu S, Xie Y, Zhao Y, Chen B, et al. Preparation and characterization of regenerated cellulose/TiO_2/ZnO nanocomposites and its photocatalytic activity. Mater Lett 2014;117. http://dx.doi.org/10.1016/j.matlet.2013.12.009.
[117] Zhu H, Jiang R, Fu Y, Guan Y, Yao J, Xiao L, et al. Effective photocatalytic decolorization of methyl orange utilizing TiO_2/ZnO/chitosan nanocomposite films under simulated solar irradiation. Desalination 2012;286:41–8. http://dx.doi.org/10.1016/j.desal.2011.10.036.
[118] Liu Y, Zhu G, Chen J, Xu H, Shen X, Yuan A. Co_3O_4/ZnO nanocomposites for gas-sensing applications. Appl Surf Sci 2013;265:379–84. http://dx.doi.org/10.1016/j.apsusc.2012.11.016.
[119] Huang Y, Wei Y, Wu J, Guo C, Wang M, Yin S, et al. Low temperature synthesis and photocatalytic properties of highly oriented ZnO/$TiO_{2-x}N_y$ coupled photocatalysts. Appl Catal B Environ 2012;123:9–17. http://dx.doi.org/10.1016/j.apcatb.2012.04.010.
[120] Wang C, Wang X, Xu B-Q, Zhao J, Mai B, Peng P, et al. Enhanced photocatalytic performance of nanosized coupled ZnO/SnO_2 photocatalysts for methyl orange degradation. J Photochem Photobiol A Chem 2004;168:47–52. http://dx.doi.org/10.1016/j.jphotochem.2004.05.014.
[121] Chang X, Li Z, Zhai X, Sun S, Gu D, Dong L, et al. Efficient synthesis of sunlight-driven ZnO-based heterogeneous photocatalysts. Mater Des 2016;98:324–32. http://dx.doi.org/10.1016/j.matdes.2016.03.027.
[122] Fan H, Zhao X, Yang J, Shan X, Yang L, Zhang Y, et al. ZnO–graphene composite for photocatalytic degradation of methylene blue dye. Catal Commun 2012;29. http://dx.doi.org/10.1016/j.catcom.2012.09.013.
[123] Iftekhar Uddin ASM, Phan D-T, Chung G-S. Low temperature acetylene gas sensor based on Ag nanoparticles-loaded ZnO-reduced graphene oxide hybrid. Sens Actuators B Chem 2015;207:362–9. http://dx.doi.org/10.1016/j.snb.2014.10.091.
[124] Stoller MD, Park S, Zhu Y, An J, Ruoff RS. Graphene-based ultracapacitors. Nano Lett 2008;8:3498–502. http://dx.doi.org/10.1021/nl802558y.
[125] Balandin AA, Ghosh S, Bao W, Calizo I, Teweldebrhan D, Miao F, et al. Superior thermal conductivity of single-layer graphene. Nano Lett 2008;8:902–7. http://dx.doi.org/10.1021/nl0731872.
[126] Bolotin KI, Sikes KJ, Jiang Z, Klima M, Fudenberg G, Hone J, et al. Ultrahigh electron mobility in suspended graphene. Solid State Commun 2008;146. http://dx.doi.org/10.1016/j.ssc.2008.02.024.
[127] Lee C, Wei X, Kysar JW, Hone J. Measurement of the elastic properties and intrinsic strength of monolayer graphene. Science 2008;80-:321.
[128] Paulchamy B, Arthi G. A simple approach to stepwise synthesis of graphene oxide nanomaterial. J Nanomed 2015.
[129] Li B, Liu T, Wang Y, Wang Z. ZnO/graphene-oxide nanocomposite with remarkably enhanced visible-light-driven photocatalytic performance. J Colloid Interface Sci 2012;377:114–21. http://dx.doi.org/10.1016/j.jcis.2012.03.060.
[130] Liu Y, Hu Y, Zhou M, Qian H, Hu X. Microwave-assisted non-aqueous route to deposit well-dispersed ZnO nanocrystals on reduced graphene oxide sheets with improved photoactivity for the decolorization of dyes under visible light. Appl Catal B Environ 2012;125:425–31. http://dx.doi.org/10.1016/j.apcatb.2012.06.016.
[131] Fu D, Han G, Yang F, Zhang T, Chang Y, Liu F. Seed-mediated synthesis and the photo-degradation activity of ZnO–graphene hybrids excluding the influence of dye adsorption. Appl Surf Sci 2013;283:654–9. http://dx.doi.org/10.1016/j.apsusc.2013.07.003.
[132] Liu S, Sun H, Liu S, Wang S. Graphene facilitated visible light photodegradation of methylene blue over titanium dioxide photocatalysts. Chem Eng J 2013;214:298–303. http://dx.doi.org/10.1016/j.cej.2012.10.058.
[133] Zhou X, Shi T, Zhou H. Hydrothermal preparation of ZnO-reduced graphene oxide hybrid with high performance in photocatalytic degradation. Appl Surf Sci 2012;258:6204–11. http://dx.doi.org/10.1016/j.apsusc.2012.02.131.
[134] Bosch-Navarro C, Coronado E, Martí-Gastaldo C, Sánchez-Royo JF, Gómez MG. Influence of the pH on the synthesis of reduced graphene oxide under hydrothermal conditions. Nanoscale 2012;4:3977. http://dx.doi.org/10.1039/c2nr30605k.
[135] Steplin Paul Selvin S, Radhika N, Borang O, Sharmila Lydia I, Princy Merlin J. Visible light driven photodegradation of Rhodamine B using cysteine capped ZnO/GO nanocomposite as photocatalyst. J Mater Sci Mater Electron 2017:1–9. http://dx.doi.org/10.1007/s10854-017-6367-y.
[136] Zhang Y, Mu J. Controllable synthesis of flower- and rod-like ZnO nanostructures by simply tuning the ratio of sodium hydroxide to zinc acetate. Nanotechnology 2007;18:75606. http://dx.doi.org/10.1088/0957-4484/18/7/075606.
[137] Gupta J, Barick KC, Bahadur D. Defect mediated photocatalytic activity in shape-controlled ZnO nanostructures. J Alloy Compd 2011;509:6725–30. http://dx.doi.org/10.1016/j.jallcom.2011.03.157.
[138] Akir S, Barras A, Coffinier Y, Bououdina M, Boukherroub R, Omrani AD. Eco-friendly synthesis of ZnO nanoparticles with different morphologies and their visible light photocatalytic performance for the degradation of Rhodamine B. Ceram Int 2016;42:10259–65. http://dx.doi.org/10.1016/j.ceramint.2016.03.153.
[139] Becker J, Raghupathi KR, St. Pierre J, Zhao D, Koodali RT. Tuning of the crystallite and particle sizes of ZnO nanocrystalline materials in solvothermal synthesis and their photocatalytic activity for dye degradation. J Phys Chem C 2011;115:13844–50. http://dx.doi.org/10.1021/jp2038653.
[140] Ong CB, Mohammad AW, Rohani R, Ba-Abbad MM, Hairom NHH. Solar photocatalytic degradation of hazardous Congo red using low-temperature synthesis of zinc oxide nanoparticles. Process Saf Environ Prot 2017;104:549–57. http://dx.doi.org/10.1016/j.psep.2016.04.006.
[141] Hong R, Pan T, Qian J, Li H. Synthesis and surface modification of ZnO nanoparticles. Chem Eng J 2006;119:71–81. http://dx.doi.org/10.1016/j.cej.2006.03.003.
[142] Farzi GA, Tayebee R, Naghibinasab S. Surface modification of ZnO nano-particles with trimetoxyvinyl silane and oleic acid and studying their dispersion in organic media. Int J Nano Dimens 2015;6:67–75. http://dx.doi.org/10.7508/IJND.2015.06.009.
[143] Sperling RA, Parak WJ. Surface modification, functionalization and bioconjugation of colloidal inorganic nanoparticles. Philos Trans R Soc Lond A Math Phys Eng Sci 2010:368.
[144] Zhang X, Xia Y, He T. Tuning photoluminescence properties of ZnO nanorods via surface modification. Mater Chem Phys 2012;137:622–7. http://dx.doi.org/10.1016/j.matchemphys.2012.09.065.
[145] Hong RY, Li JH, Chen LL, Liu DQ, Li HZ, Zheng Y, et al. Synthesis, surface modification and photocatalytic property of ZnO nanoparticles. Powder Technol 2009;189:426–32. http://dx.doi.org/10.1016/j.powtec.2008.07.004.
[146] Luo J, Dai X, Bai S, Jin Y, Ye Z, Guo X. Ligand exchange of colloidal ZnO nanocrystals from the high temperature and nonaqueous approach. Nano-Micro Lett 2013;5:274–80. http://dx.doi.org/10.1007/BF03353758.
[147] Kwon D, Park J, Park J, Choi SY, Yoon TH. Effects of surface-modifying ligands on the colloidal stability of ZnO nanoparticle dispersions in in vitro cytotoxicity test media. Int J Nanomed 2014;9(Suppl. 2):S57–S65. http://dx.doi.org/10.2147/IJN.S57924.
[148] Kango S, Kalia S, Celli A, Njuguna J, Habibi Y, Kumar R. Surface modification of inorganic nanoparticles for development of organic–inorganic nanocomposites—a review. Prog Polym Sci 2013;38:1232–61. http://dx.doi.org/10.1016/j.progpolymsci.2013.02.003.
[149] Kuriakose S, Bhardwaj N, Singh J, Satpati B, Mohapatra S. Structural, optical and photocatalytic properties of flower-like ZnO nanostructures prepared by a facile wet chemical method. Beilstein J Nanotechnol 2013;4:763–70. http://dx.doi.org/10.3762/bjnano.4.87.
[150] Ong W-J, Voon S-Y, Tan L-L, Goh BT, Yong S-T, Chai S-P. Enhanced daylight-induced photocatalytic activity of solvent exfoliated graphene (SEG)/ZnO hybrid nanocomposites toward degradation of Reactive Black 5. Ind Eng Chem Res 2014;53:17333–44. http://dx.doi.org/10.1021/ie5027088.
[151] Rong MZ, Zhang MQ, Zheng YX, Zeng HM, Walter R, Friedrich K. Structure–property relationships of irradiation grafted nano-inorganic particle filled polypropylene composites. Polymer 2001;42:167–83. http://dx.doi.org/10.1016/S0032-3861(00)00325-6.

[152] Mahmood MA, Baruah S, Dutta J. Enhanced visible light photocatalysis by manganese doping or rapid crystallization with ZnO nanoparticles. Mater Chem Phys 2011;130:531–5. http://dx.doi.org/10.1016/j.matchemphys.2011.07.018.
[153] Umar K, Aris A, Parveen T, Jaafar J, Abdul Majid Z, Vijaya Bhaskar Reddy A, et al. Synthesis, characterization of Mo and Mn doped ZnO and their photocatalytic activity for the decolorization of two different chromophoric dyes. Appl Catal A Gen 2015;505:507–14. http://dx.doi.org/10.1016/j.apcata.2015.02.001.
[154] Ullah R, Dutta J. Photocatalytic degradation of organic dyes with manganese-doped ZnO nanoparticles. J Hazard Mater 2008;156:194–200. http://dx.doi.org/10.1016/j.jhazmat.2007.12.033.
[155] Rekha K, Nirmala M, Nair MG, Anukaliani A. Structural, optical, photocatalytic and antibacterial activity of zinc oxide and manganese doped zinc oxide nanoparticles. Phys B Condens Matter 2010;405:3180–5. http://dx.doi.org/10.1016/j.physb.2010.04.042.
[156] Jongnavakit P, Amornpitoksuk P, Suwanboon S, Ndiege N. Preparation and photocatalytic activity of Cu-doped ZnO thin films prepared by the sol–gel method. Appl Surf Sci 2012;258:8192–8. http://dx.doi.org/10.1016/j.apsusc.2012.05.021.
[157] Fu M, Li Y, Wu S, Lu P, Liu J, Dong F. Sol–gel preparation and enhanced photocatalytic performance of Cu-doped ZnO nanoparticles. Appl Surf Sci 2011;258:1587–91. http://dx.doi.org/10.1016/j.apsusc.2011.10.003.
[158] Thennarasu G, Sivasamy A. Enhanced visible photocatalytic activity of cotton ball like nano structured Cu doped ZnO for the degradation of organic pollutant. Ecotoxicol Environ Saf 2016;134:412–20. http://dx.doi.org/10.1016/j.ecoenv.2015.10.030.
[159] Mittal M, Sharma M, Pandey OP. UV–Visible light induced photocatalytic studies of Cu doped ZnO nanoparticles prepared by co-precipitation method. Sol Energy 2014;110:386–97. http://dx.doi.org/10.1016/j.solener.2014.09.026.
[160] Mohan R, Krishnamoorthy K, Kim S-J. Enhanced photocatalytic activity of Cu-doped ZnO nanorods. Solid State Commun 2012;152. http://dx.doi.org/10.1016/j.ssc.2011.12.008.
[161] He R, Hocking RK, Tsuzuki T. Co-doped ZnO nanopowders: location of cobalt and reduction in photocatalytic activity. Mater Chem Phys 2012;132:1035–40. http://dx.doi.org/10.1016/j.matchemphys.2011.12.061.
[162] Shinde SS, Bhosale CH, Rajpure KY. Oxidative degradation of acid orange 7 using Ag-doped zinc oxide thin films. J Photochem Photobiol B 2012;117:262–8. http://dx.doi.org/10.1016/j.jphotobiol.2012.10.011.
[163] Whang T-J, Hsieh M-T, Chen H-H. Visible-light photocatalytic degradation of methylene blue with laser-induced Ag/ZnO nanoparticles. Appl Surf Sci 2012;258:2796–801. http://dx.doi.org/10.1016/j.apsusc.2011.10.134.
[164] Divband B, Khatamian M, Eslamian GRK, Darbandi M. Synthesis of Ag/ZnO nanostructures by different methods and investigation of their photocatalytic efficiency for 4-nitrophenol degradation. Appl Surf Sci 2013;284:80–6. http://dx.doi.org/10.1016/j.apsusc.2013.07.015.
[165] Zhong J Bo, Li J Zhang, He X Yang, Zeng J, Lu Y, Hu W, et al. Improved photocatalytic performance of Pd-doped ZnO. Curr Appl Phys 2012;12:998–1001. http://dx.doi.org/10.1016/j.cap.2012.01.003.
[166] Khalil A, Gondal MA, Dastageer MA. Augmented photocatalytic activity of palladium incorporated ZnO nanoparticles in the disinfection of Escherichia coli microorganism from water. Appl Catal A Gen 2011;402:162–7. http://dx.doi.org/10.1016/j.apcata.2011.05.041.
[167] Sanoop PK, Anas S, Ananthakumar S, Gunasekar V, Saravanan R, Ponnusami V. Synthesis of yttrium doped nanocrystalline ZnO and its photocatalytic activity in methylene blue degradation. Arab J Chem 2016;9:S1618–S1626. http://dx.doi.org/10.1016/j.arabjc.2012.04.023.
[168] Ahmad M, Ahmed E, Hong ZL, Iqbal Z, Khalid NR, Abbas T, et al. Structural, optical and photocatalytic properties of hafnium doped zinc oxide nanophotocatalyst. Ceram Int 2013;39:8693–700. http://dx.doi.org/10.1016/j.ceramint.2013.04.051.
[169] Wang Y, Zhao X, Duan L, Wang F, Niu H, Guo W, et al. Structure, luminescence and photocatalytic activity of Mg-doped ZnO nanoparticles prepared by auto combustion method. Mater Sci Semicond Process 2015;29:372–9. http://dx.doi.org/10.1016/j.mssp.2014.07.034.
[170] Selvam NCS, Narayanan S, Kennedy LJ, Vijaya JJ. Pure and Mg-doped self-assembled ZnO nano-particles for the enhanced photocatalytic degradation of 4-chlorophenol. J Environ Sci 2013;25:2157–67.
[171] Ivetić TB, Dimitrievska MR, Finčur NL, Đačanin LR, Gúth IO, Abramović BF, et al. Effect of annealing temperature on structural and optical properties of Mg-doped ZnO nanoparticles and their photocatalytic efficiency in alprazolam degradation. Ceram Int 2014;40:1545–52. http://dx.doi.org/10.1016/j.ceramint.2013.07.041.
[172] Jia X, Fan H, Afzaal M, Wu X, O'Brien P. Solid state synthesis of tin-doped ZnO at room temperature: characterization and its enhanced gas sensing and photocatalytic properties. J Hazard Mater 2011;193:194–9. http://dx.doi.org/10.1016/j.jhazmat.2011.07.049.
[173] Kaneva NV, Dimitrov DT, Dushkin CD. Effect of nickel doping on the photocatalytic activity of ZnO thin films under UV and visible light. Appl Surf Sci 2011;257:8113–20. http://dx.doi.org/10.1016/j.apsusc.2011.04.119.
[174] Zhong J Bo, Li J Zhang, Lu Y, He X Yang, Zeng J, Hu W, et al. Fabrication of Bi^{3+}-doped ZnO with enhanced photocatalytic performance. Appl Surf Sci 2012;258:4929–33. http://dx.doi.org/10.1016/j.apsusc.2012.01.121.
[175] Su CY, Lu CT, Hsiao WT, Liu WH, Shieu FS. Evaluation of the microstructural and photocatalytic properties of aluminum-doped zinc oxide coatings deposited by plasma spraying. Thin Solid Films 2013;544:170–4. http://dx.doi.org/10.1016/j.tsf.2013.03.129.
[176] Faisal M, Ismail AA, Ibrahim AA, Bouzid H, Al-Sayari SA. Highly efficient photocatalyst based on Ce doped ZnO nanorods: controllable synthesis and enhanced photocatalytic activity. Chem Eng J 2013;229:225–33. http://dx.doi.org/10.1016/j.cej.2013.06.004.
[177] Karunakaran C, Gomathisankar P, Manikandan G. Preparation and characterization of antimicrobial Ce-doped ZnO nanoparticles for photocatalytic detoxification of cyanide. Mater Chem Phys 2010;123:585–94. http://dx.doi.org/10.1016/j.matchemphys.2010.05.019.
[178] Kumar S, Sahare PD. Nd-doped ZnO as a multifunctional nanomaterial. J Rare Earths 2012;30:761–8. http://dx.doi.org/10.1016/S1002-0721(12)60126-4.
[179] Zhao Z, Song J, Zheng J, Lian J. Optical properties and photocatalytic activity of Nd-doped ZnO powders. Trans Nonferrous Met Soc China 2014;24:1434–9. http://dx.doi.org/10.1016/S1003-6326(14)63209-X.
[180] Zong Y, Li Z, Wang X, Ma J, Men Y. Synthesis and high photocatalytic activity of Eu-doped ZnO nanoparticles. Ceram Int 2014;40:10375–82. http://dx.doi.org/10.1016/j.ceramint.2014.02.123.
[181] Sin J-C, Lam S-M, Lee K-T, Mohamed AR. Photocatalytic performance of novel samarium-doped spherical-like ZnO hierarchical nanostructures under visible light irradiation for 2,4-dichlorophenol degradation. J Colloid Interface Sci 2013;401:40–9. http://dx.doi.org/10.1016/j.jcis.2013.03.043.
[182] Sin J-C, Lam S-M, Lee K-T, Mohamed AR. Preparation and photocatalytic properties of visible light-driven samarium-doped ZnO nanorods. Ceram Int 2013;39:5833–43. http://dx.doi.org/10.1016/j.ceramint.2013.01.004.
[183] Suwanboon S, Amornpitoksuk P, Sukolrat A, Muensit N. Optical and photocatalytic properties of La-doped ZnO nanoparticles prepared via precipitation and mechanical milling method. Ceram Int 2013;39:2811–9. http://dx.doi.org/10.1016/j.ceramint.2012.09.050.
[184] Anandan S, Vinu A, Sheeja Lovely KLP, Gokulakrishnan N, Srinivasu P, Mori T, et al. Photocatalytic activity of La-doped ZnO for the degradation of monocrotophos in aqueous suspension. J Mol Catal A Chem 2007;266:149–57. http://dx.doi.org/10.1016/j.molcata.2006.11.008.
[185] Khataee A, Soltani RDC, Karimi A, Joo SW. Sonocatalytic degradation of a textile dye over Gd-doped ZnO nanoparticles synthesized through sonochemical process. Ultrason Sonochem 2015;23:219–30. http://dx.doi.org/10.1016/j.ultsonch.2014.08.023.
[186] Haibo O, Feng HJ, Cuiyan L, Liyun C, Jie F. Synthesis of carbon doped ZnO with a porous structure and its solar-light photocatalytic properties. Mater Lett 2013;111. http://dx.doi.org/10.1016/j.matlet.2013.08.081.
[187] Patil AB, Patil KR, Pardeshi SK. Ecofriendly synthesis and solar photocatalytic activity of S-doped ZnO. J Hazard Mater 2010;183:315–23. http://dx.doi.org/10.1016/j.jhazmat.2010.07.026.
[188] Wu C. Facile one-step synthesis of N-doped ZnO micropolyhedrons for efficient photocatalytic degradation of formaldehyde under visible-light irradiation. Appl Surf Sci 2014;319:237–43. http://dx.doi.org/10.1016/j.apsusc.2014.04.217.
[189] Rajbongshi BM, Ramchiary A, Samdarshi S. Influence of N-doping on photocatalytic activity of ZnO nanoparticles under visible light irradiation. Mater Lett 2014;134. http://dx.doi.org/10.1016/j.matlet.2014.07.073.
[190] Gu P, Wang X, Li T, Meng H. Investigation of defects in N-doped ZnO powders prepared by a facile solvothermal method and their UV photocatalytic properties. Mater Res Bull 2013;48:4699–703. http://dx.doi.org/10.1016/j.materresbull.2013.08.034.
[191] Prieto-Rodriguez L, Miralles-Cuevas S, Oller I, Agüera A, Puma GL, Malato S. Treatment of emerging contaminants in wastewater treatment plants (WWTP) effluents by solar photocatalysis using low TiO2 concentrations. J Hazard Mater 2012;211:131–7. http://dx.doi.org/10.1016/j.jhazmat.2011.09.008.
[192] Han J, Liu Y, Singhal N, Wang L, Gao W. Comparative photocatalytic degradation of estrone in water by ZnO and TiO_2 under artificial UVA and solar irradiation. Chem Eng J 2012;213:150–62. http://dx.doi.org/10.1016/j.cej.2012.09.066.
[193] Sarasidis VC, Plakas KV, Patsios SI, Karabelas AJ. Investigation of diclofenac degradation in a continuous photo-catalytic membrane reactor. Influence of operating parameters. Chem Eng J 2014;239:299–311. http://dx.doi.org/10.1016/j.cej.2013.11.026.
[194] Hairom NHH, Mohammad AW, Kadhum AAH. Effect of various zinc oxide nanoparticles in membrane photocatalytic reactor for Congo red dye treatment. Sep Purif Technol 2014;137:74–81. http://dx.doi.org/10.1016/j.seppur.2014.09.027.
[195] Mozia S. Photocatalytic membrane reactors (PMRs) in water and wastewater treatment. A review. Sep Purif Technol 2010;73:71–91. http://dx.doi.org/10.1016/j.seppur.2010.03.021.
[196] Song H, Shao J, He Y, Liu B, Zhong X. Natural organic matter removal and flux decline with PEG–TiO_2-doped PVDF membranes by integration of ultrafiltration with photocatalysis. J Memb Sci 2012;405:48–56. http://dx.doi.org/10.1016/j.memsci.2012.02.063.
[197] Zhang X, Wang DK, Diniz da Costa JC. Recent progresses on fabrication of photocatalytic membranes for water treatment. Catal Today 2014;230:47–54. http://dx.doi.org/10.1016/j.cattod.2013.11.019.
[198] Kim J, Van der Bruggen B. The use of nanoparticles in polymeric and ceramic membrane structures: review of manufacturing procedures and performance improvement for water treatment. Environ Pollut 2010;158:2335–49. http://dx.doi.org/10.1016/j.envpol.2010.03.024.
[199] Song H, Shao J, Wang J, Zhong X. The removal of natural organic matter with LiCl–TiO_2-doped PVDF membranes by integration of ultrafiltration with photocatalysis. Desalination 2014;344:412–21. http://dx.doi.org/10.1016/j.desal.2014.04.012.
[200] Hu B, Zhou J, Wu X-M. Decoloring methyl orange under sunlight by a photocatalytic membrane reactor based on ZnO nanoparticles and polypropylene macroporous membrane. Int J Polym Sci 2013;2013:1–8. http://dx.doi.org/

10.1155/2013/451398.
[201] Mascolo G, Comparelli R, Curri ML, Lovecchio G, Lopez A, Agostiano A. Photocatalytic degradation of methyl red by TiO_2: comparison of the efficiency of immobilized nanoparticles versus conventional suspended catalyst. J Hazard Mater 2007;142:130–7. http://dx.doi.org/10.1016/j.jhazmat.2006.07.068.
[202] Kacem M, Plantard G, Wery N, Goetz V. Kinetics and efficiency displayed by supported and suspended TiO_2 catalysts applied to the disinfection of Escherichia coli. Chin J Catal 2014;35:1571–7. http://dx.doi.org/10.1016/S1872-2067(14)60212-6.
[203] Brezova V, Jankovičová M, Soldan M. Photocatalytic degradation of p-toluene-sulphonic acid in aqueous systems containing powdered and immobilized titanium dioxide. J Photochem Photobiol A 1994;83(1):69–75.
[204] Mansilla HD, Bravo C, Ferreyra R, Litter MI, Jardim WF, Lizama C, et al. Photocatalytic EDTA degradation on suspended and immobilized TiO_2. J Photochem Photobiol A Chem 2006;181:188–94. http://dx.doi.org/10.1016/j.jphotochem.2005.11.023.
[205] Dijkstra MF, Michorius A, Buwalda H, Panneman H, Winkelman JG, Beenackers AAC. Comparison of the efficiency of immobilized and suspended systems in photocatalytic degradation. Catal Today 2001;66:487–94. http://dx.doi.org/10.1016/S0920-5861(01)00257-7.